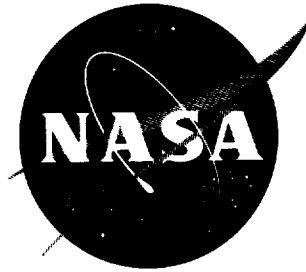


46p.

N62-16705-

NASA TN D-1348

NASA TN D-1348



TECHNICAL NOTE

D-1348

SPACECRAFT INFORMATION SYSTEMS

George H. Ludwig

Goddard Space Flight Center
Greenbelt, Maryland

NATIONAL AERONAUTICS AND SPACE ADMINISTRATION
WASHINGTON

October 1962

SPACECRAFT INFORMATION SYSTEMS

by

George H. Ludwig

Goddard Space Flight Center

SUMMARY

To obtain the greatest benefit from a satellite or space probe experiment, the effects of the complete spacecraft information system on these data must be considered. This system includes the detectors, the signal conditioning equipment, the telemetry link, the data reduction equipment, and the method of data display. This report reviews the present state of the art of instrumentation for cosmic ray, solar proton, solar plasma, and geomagnetically trapped radiation experiments.

The detector arrays and the instrumentation required to condition the signals from the detectors are steadily growing more complex to permit more meaningful and accurate measurements. A sampling of present basic linear and logic circuits is examined, and several spacecraft systems are discussed to illustrate the combining of these fundamental circuits. The telemetry link and the operational requirements of an active spacecraft are discussed, and the necessity for adequate data handling facilities on the ground is emphasized.

CONTENTS

Summary	i
INTRODUCTION	1
GENERAL CONSIDERATIONS	3
BASIC CIRCUITS	6
SIMPLE SUBSYSTEMS	14
COMPLETE SIGNAL CONDITIONING SYSTEMS	15
ADVANCED SPACECRAFT CENTRAL DATA	
HANDLING SYSTEMS	23
TELEMETRY	26
ENCODING AND DETECTION	35
DATA RECOVERY	37
DATA REDUCTION	39
CONCLUDING REMARKS	41
References	42

SPACECRAFT INFORMATION SYSTEMS[†]

by

George H. Ludwig

Goddard Space Flight Center

INTRODUCTION

The value of earth satellites and space probes for gathering scientific information about the physical universe is well established. Since these spacecraft are very expensive, it is necessary that considerable thought be given to maximizing the amount of information which can be obtained from each one. This report contains a discussion of some of the difficulties involved in conducting an experiment in space and some of the techniques which are available for this purpose.

Any experiment, no matter where it is conducted, may be thought of as a generalized system as shown in Figure 1. The end elements are the basic sensors and the final

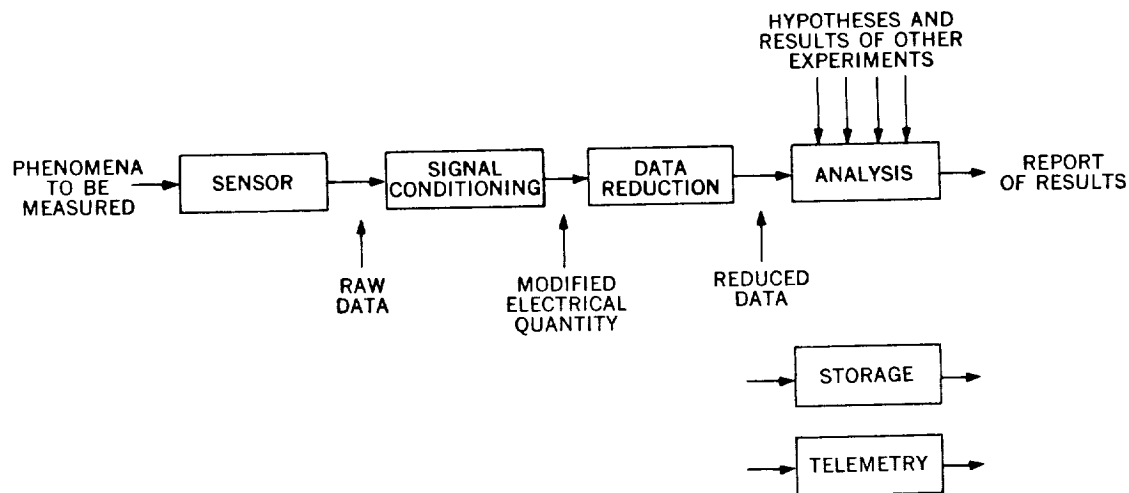


Figure 1 — General outline of the elements and information flow of an experiment

[†]This paper was presented as part of the course on Cosmic Radiation, Solar Particles, and Space Research, Scuola Internazionale di Fisica "Enrico Fermi", Varenna sul Lago di Como, Italy, on May 23–June 3, 1961.

report of results. The intermediate elements are the signal conditioning instruments, which convert the signals from the basic sensors into usable electrical quantities, the process of reduction of these electrical quantities into a form which can be used by the experimenter, and the analysis of the data. In addition, for many experiments it is necessary to add storage in one or in several places. (Storage may actually be a part of all the blocks in Figure 1.) For example, if the sensor is a self-integrating ion chamber of the Neher type, it provides a storage function of its own. If the pulses appearing at the output of this chamber are counted, then this counter represents a second form of storage. A tape recorder is often incorporated into the signal conditioning and data reduction systems; and the placing of the reduced data on an oscillograph record or in tabular form is also storage.

The major difference between the general outline shown in Figure 1 and a spacecraft system is the addition of a block representing the telemetering of the data from the spacecraft to the earth. This block can, in principle, be placed anywhere along the line of data flow. In general, the information bit rate along this line decreases as one progresses from the left to the right end of the diagram. It must be remembered that the experimenter may see his data for the first time at the output of the telemetry system. The factors which determine where the telemetry system should be placed along the line of data flow for any specific experiment include:

1. *The ability of the experimenter to predict the results.* If the experimenter knows where in the possible range of values his results will occur, he may arrange for considerable processing in the satellite before he sees the data. If, for example, he is measuring the energy spectrum of protons in the cosmic ray flux, and if he already has a general idea of the energy spectra of all the constituents, he might concentrate on the protons and reject all other particles. He might go so far as to include a computer in the spacecraft to determine an analytic function that would represent the spectrum. Then he would need to telemeter only a set of coefficients rather than an extensive set of data points. On the other hand, if very little is known about the phenomenon, it may be necessary to telemeter all data directly from the sensor and then, after a preliminary investigation of the raw data on the ground, to determine how they should be conditioned and reduced.

2. *System reliability.* The larger the amount of data processing in the spacecraft, the greater is the complexity and the smaller the reliability of the system. If the experimenter were to telemeter only the coefficients discussed above, he would need to have a high degree of confidence in his instrumentation.

3. *Information bandwidth available for data transmission.* Obviously, the first alternative discussed under (1) above would require far less information bandwidth than the second.

4. *Time available for the preparation of the experiments.* Complex spacecraft data processing systems require a long time for development and calibration.

Obviously, the best location along the line of data flow for placement of the telemetry system can vary widely, even among experiments on the same spacecraft. Thus, any acceptable central spacecraft data handling system must be carefully designed to permit the necessary flexibility.

GENERAL CONSIDERATIONS

On spacecraft containing more than one experiment, the signal conditioning instrumentation is often split into two sections. The first section consists of the detectors and the circuits which process their outputs up to the point where the central system combines the data from a number of experiments. The second section includes the instrumentation in the central system, which may further process and store the data before transmission. As attempts are made to measure the characteristics of the phenomena in greater and greater detail, more and more data processing in the spacecraft before transmission will become necessary. This trend is expected to continue to the point where programmable computers will be used aboard the spacecraft to perform complex analyses. This results from the fact that the computers will require less payload weight than will be required to meet the electrical power demands of telemetering very large quantities of raw data, and that conservation of ground receiving station capabilities and data reduction facilities will be necessary.

Many different detectors exist for studying energetic particles. Table 1 lists them and indicates their applicability for use on spacecraft. Most of these detectors rely on the process of ionization for operation: The particle being detected produces ionization in the detector and the electrons, ions, and photons which result are gathered and analyzed. Some of the characteristics of the electrical signals which appear at the detector outputs are also summarized in Table 1. These are the signals which must be prepared for storage and transmission over the telemetry link by the signal conditioning instrumentation.

The raw information must be converted into a form which is the most meaningful form practicable, and capable of being transmitted over a telemetry link. Also:

1. The telemetry must be accomplished within the smallest information bandwidth practicable.
2. The instrumentation must meet the requirements of ruggedness, relatively low operating power, light weight, and relatively small volume imposed by the launching vehicle capabilities and the launching environment.

Table 1
Energetic Charged Particle Detectors

Detector Type	Physical Process Used	Form(s) of Output	Characteristic(s) of Output Used	Use in U. S. Satellites
Ion Chamber	Ionization of a gas	Pulse	Pulse rate	Used in Pioneer I, V, Explorer VI, VII
		Integrated current	Charge per pulse Charge per unit time	
Proportional Counter	Ionization of a gas and ion multiplication	Pulse	Pulse rate Charge per pulse	Used in Pioneer V, Explorer VI
Geiger-Müller Counter	Ionization of a gas and ion multiplication	Pulse Integrated current	Pulse rate Charge per unit time	Used in Explorer I, III, IV, VI, VII, XII, Pioneer I, III, IV, V
Cloud Chamber	Ionization and condensation in a super-saturated gas	Visual tracks, recorded by a photographic film or television system	Rate of events	Not presently feasible because of need for film recovery or transmission of high resolution pictures
			Ionization density along track Curvature of track when magnetic or electric fields are applied Study of sequence of interactions and secondary particles produced	
Bubble Chamber	Ionization and vaporization in a superheated liquid	Same as cloud chamber	Same as cloud chamber	Same as cloud chamber
Solid Chamber	Solid scintillator followed by image intensifier and picture system	Same as cloud chamber	Same as cloud chamber	Same as cloud chamber

Table 1 (Continued)

Detector Type	Physical Process Used	Form(s) of Output	Characteristic(s) of Output Used	Use in U. S. Satellites
Nuclear Emulsions	Ionization by particles produces developable silver halide grains	Visual tracks in body of emulsion usually observed under microscope	Same as cloud chamber	Requires emulsion recovery. Used in SBE, NERV, Atlas pod rocket firings
Ion Collector	Direct interception of low energy charged particles	Pulse	Pulse rate	Used in Explorer X, XII
		Integrated current	Charge per pulse	
			Charge per unit time	
Scintillation Detector	Ionization or excitation of atoms in a gas, liquid, or solid and production of photons during de-excitation. Detection of photons by light sensitive detector such as photo-multiplier tube	Pulse	Pulse rate	Used in Explorer IV, VI, XI, XII Pioneer V
			Pulse shape	
		Integrated current	P.M. Charge per pulse	
Cerenkov Detector	Cerenkov radiation in a gas, liquid, or solid. Detection of the photons by light-sensitive detector such as photo-multiplier tube	Pulse	P.M. Charge per unit time	Used in Explorer XI
			Pulse rate	
			P.M. Charge per pulse	
Solid State Detector	Ionization of atoms in a solid with resultant change of body conductivity	Resistance	Direction of propagation of photons	Used in Explorer XII, Injun I
			Conductivity	
			Pulse rate	
			Voltage amplitude of pulse	
	Ionization of atoms in a solid and transport of resultant electrons across a potential barrier (p-n junction)	Pulse		Used in Injun I

3. The instrumentation must be reliable while operating unattended for long periods in the space environment.

The operations most often performed on the outputs of detectors which are basically electronic in nature include logic operations (coincidence, anti-coincidence, etc.), pulse shaping, impedance transformation, event counting, time interval measurement, sorting, amplification (either linear or nonlinear and of either pulses or analog quantities), conversion from analog to digital form, and storage.

BASIC CIRCUITS

Many experiments use a number of individual detectors in arrays. The outputs of these detectors are often acted upon by logic circuits. It is convenient to represent the logic operations by a special symbolic language known as Boolean algebra (Reference 1). In this language:

$AB = C$ represents the logic operation "output C if A and B",

$A + B = C$ represents the operation "output C if A or B",

$\bar{A} = B$ represents the operation "B if not A".

The operations AB and $A + B$ are accomplished by the use of AND and OR logic circuits, as shown in Table 2. Commutative, associative, and distributive laws hold for these operations as follows:

Commutative laws: $AB = BA$

$$A + B = B + A$$

Associative laws: $A(BC) = (AB)C$

$$A + (B + C) = (A + B) + C$$

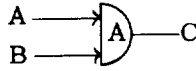
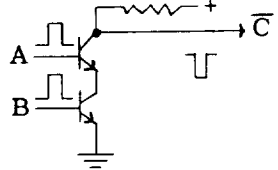
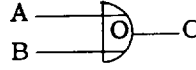
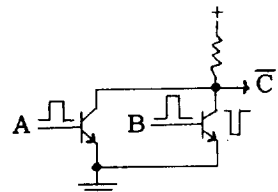
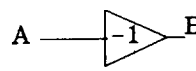
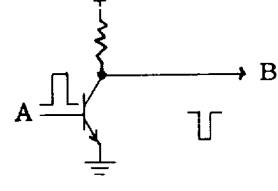
Distributive laws: $A(B + C) = AB + AC$

$$A + (BC) = (A + B)(A + C)$$

By the use of these laws and Table 2, it is possible to describe any logic system in terms of a symbolic expression.

A number of the detectors listed in Table 1 have pulse outputs which can be acted upon by these logic systems and by scalars with a minimum of preconditioning. For example, detectors which produce pulses having approximately fixed characteristics — such as Geiger-Müller (GM) counters — as a result of any detectable event, use nonlinear

Table 2
Logic Operations

Symbolic Form	Description	Block Diagram	Schematic Diagram
$AB = C$	C if A and B		
$A + B = C$	C if A or B		
$\bar{A} = B$	B if not A		

amplifiers and pulse shaping circuits to provide proper driving signals for later circuits and to help establish the threshold characteristics for the system. Figure 2 shows a simple pulse amplifier and shaping circuit used with GM counters to produce driving pulses for scaling circuits. It is a simple current-fed driver which produces a saturating output pulse when the GM tube discharge current passes through the base-emitter junction. This very simple circuit contains few components, but has the disadvantage that the system dead-time characteristics depend on the pulse-amplitude and dead-time characteristics of the counter; and on the pulse-amplitude threshold of the scaler input; and these in turn both depend to some extent on the supply voltages and operating temperature. The circuit of Figure 3 is a partial solution to this problem. It uses the voltage pulse obtained from the GM tube center wire to trigger a monostable multivibrator. Thus, the total dead-time is, to a first approximation, the sum of the multivibrator pulse width and recovery times. It is interesting to note that in this multivibrator circuit essentially no current flows except when a pulse occurs, because both transistors in the multivibrator are cut off in the quiescent condition and conduct only during the pulse interval.

The counting or scaling circuit shown in Figure 4 meets the requirements of simplicity and operates over a wide temperature range (References 2-5). This very simple

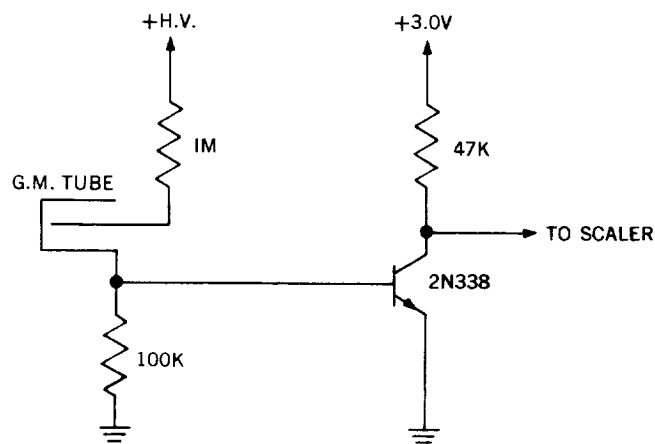


Figure 2 — A simple pulse amplifier and shaping circuit used with GM counters to produce driving pulses for scaling circuits (used in Explorers I and III by SUI)

Figure 3 — Monostable multivibrator driven by the voltage pulse obtained from the GM tube center wire. (Used in Explorer XII by GSFC)

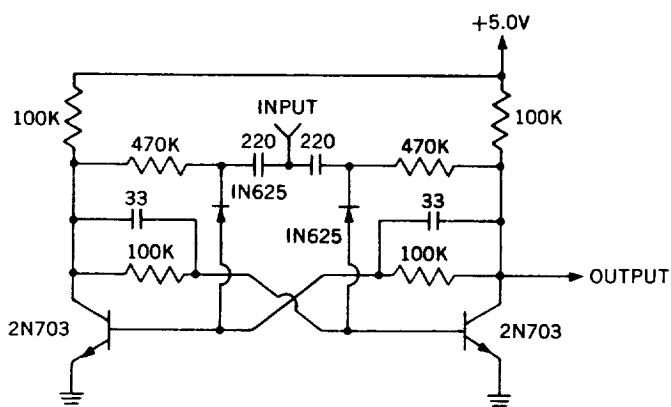
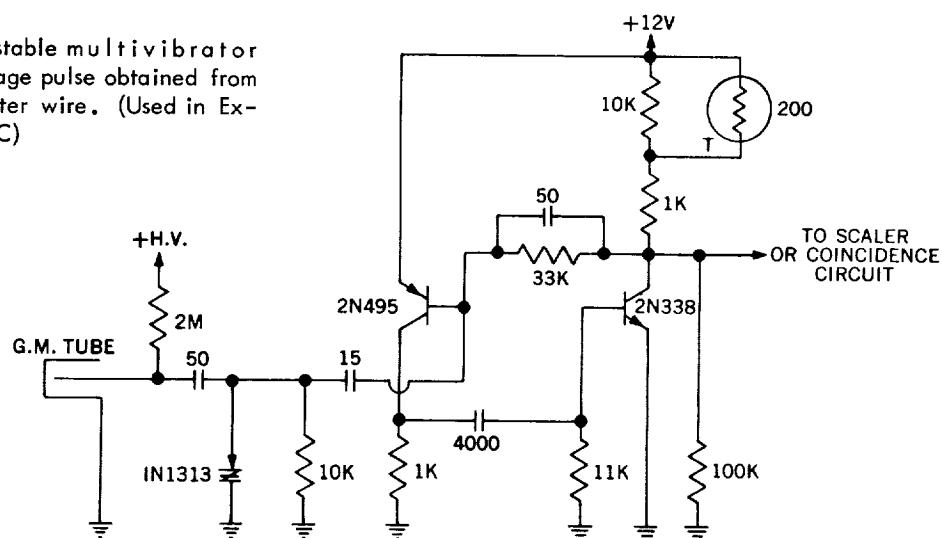


Figure 4 — Simple counting or scaling circuit (used in Explorers I, III, IV, VII, S-46†, Pioneer IV, V by SUI and U. Wisc.)

†Not successfully launched.

circuit, requiring less than a milliwatt of power per stage, can be used whenever the counting rate does not exceed 5000 per second and whenever a low output impedance is not required. Like the other scalers described below, it is capable of driving two similar circuits with no interposed circuitry. Its attractiveness lies in the relatively few components required. It operates reliably over the temperature range from -50 to $+90^{\circ}\text{C}$ and over the supply voltage range from 4.5 to 8 volts. When faster operation is necessary, a modification of this circuit can often be used, in which the pulse steering circuit time constant and the values of the collector and cross coupling resistors are halved (References 4, 5). This circuit, which operates at rates as high as 30,000 counts per second, also requires less than a milliwatt of power per stage.

When an even higher operating speed or a low output impedance is required, the complementary symmetrical scaler shown in Figure 5 can be used (Reference 6). In this circuit, the fixed collector resistors of the circuit in Figure 4 are replaced by transistors in a configuration in which one transistor is cut off and the other is conducting in each branch. Therefore, the output impedance and the current are low in both stable states. This circuit has been used at rates up to 250 kc over the temperature and voltage ranges from -30 to $+90^{\circ}\text{C}$ and 4.5 to 12 volts respectively, with a power requirement of less than 1 milliwatt per stage. Slight modifications of this circuit have been used at rates up to several megacycles per second.

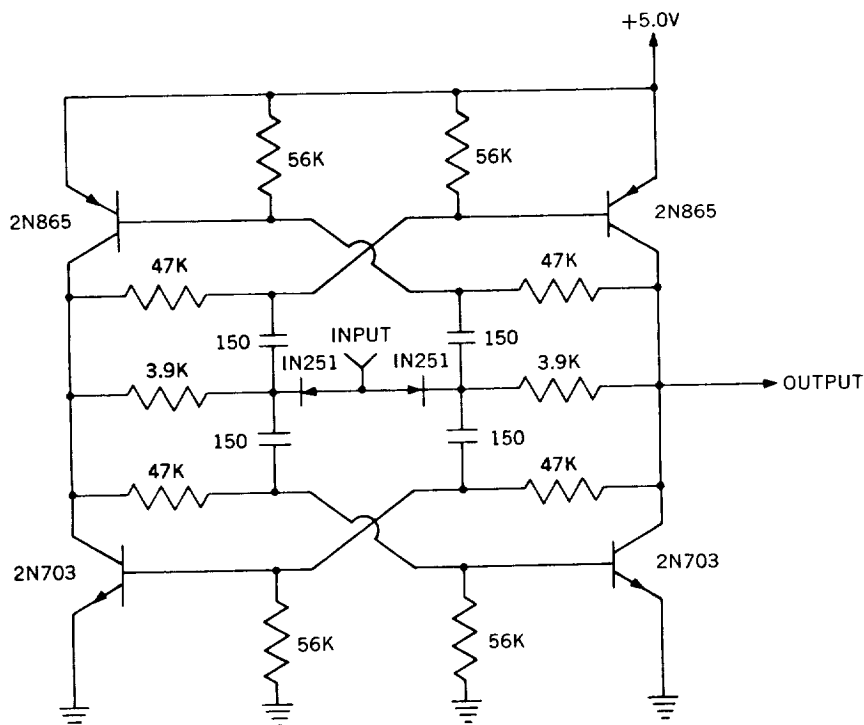


Figure 5 — Complementary symmetrical 250kc scaling circuit. (Used in Atlas-Able V, Explorer XII by GSFC)

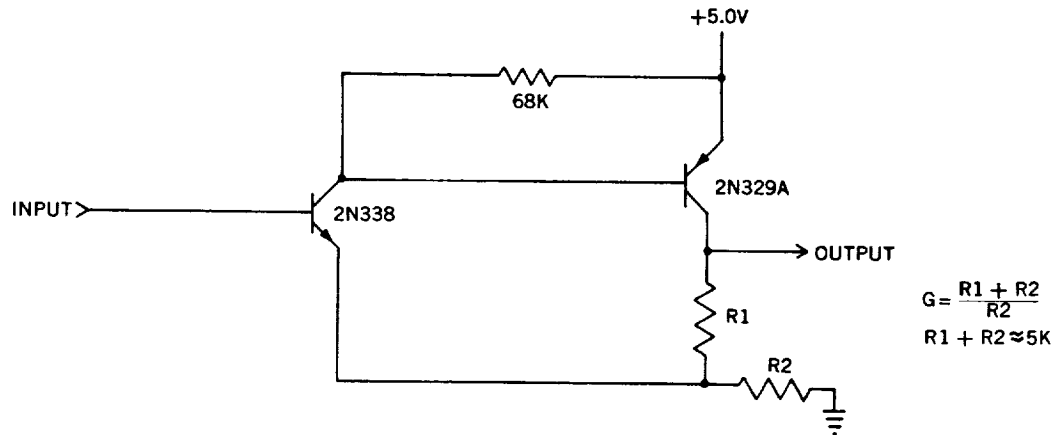


Figure 6 — Basic "bootstrap" dc coupled amplifier

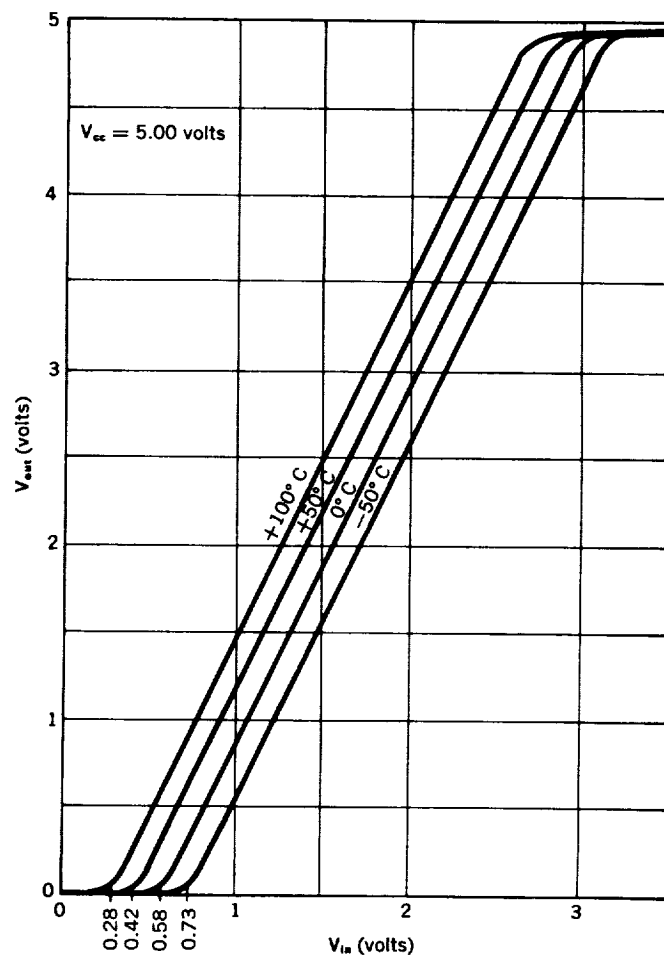


Figure 7 — Amplifier voltage gain for the basic "bootstrap" dc coupled amplifier (see Figure 6) with $G = 2$

They can be used with all pulse detectors by properly adjusting the number of stages and stage gains, and by providing suitable input circuits.

It is often necessary to convert an analog voltage or current to a digital signal. In some cases this operation can be performed in the detector itself, as in the Neher self-integrating pulse ion chamber. In this device, a coated quartz fiber is given an initial electrical charge with respect to the chamber wall by connecting it to a high voltage source. Upon receiving this charge, the fiber deflects away from the charging post. The charge on the now isolated fiber gradually leaks away because of ionization produced in the chamber by the incidence of energetic charged particles, the leakage rate depending on the rate of ionization. When the charge is nearly neutralized, the fiber again touches the charging post, acquiring a new charge and producing a pulse at the chamber output. Thus, the output pulse rate is proportional to the total rate of ionization in the chamber.

Auxiliary circuits are sometimes used to perform a similar integrated-current to pulse rate conversion. Figure 11 shows a simple relaxation oscillator used to convert current in the range 10^{-5} to 10^{-9} ampere to a pulse rate (Reference 8). This technique has been applied to measuring the current through cadmium sulfide solid state detectors, the integrated ion current in an ion chamber, and the integrated dynode current in a scintillator detector. By the proper choice of circuit components, stable operation can be obtained over a wide temperature range.

The circuit as shown in Figure 11 cannot reliably be used to measure currents smaller than 10^{-9} ampere because a current of that magnitude can leak through the discharge tube without causing a complete ionization. A simple modification of the basic circuit, however, will permit measurement of currents lower by several orders of magnitude. This is accomplished by superimposing a low amplitude periodic waveform on the discharge element. A circuit employing an auxiliary relaxation oscillator to generate this waveform is shown in Figure 12 (R. S. Rocklin, General Electric Company, private communication). It is capable of measuring currents to about 10^{-12} ampere.

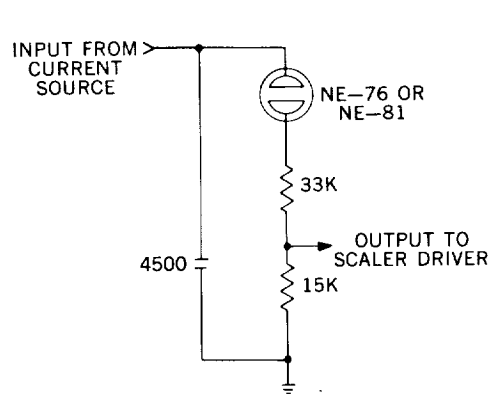


Figure 11 — Relaxation oscillator (analog-current to pulse-rate) converter (used in S-46 by SUI)

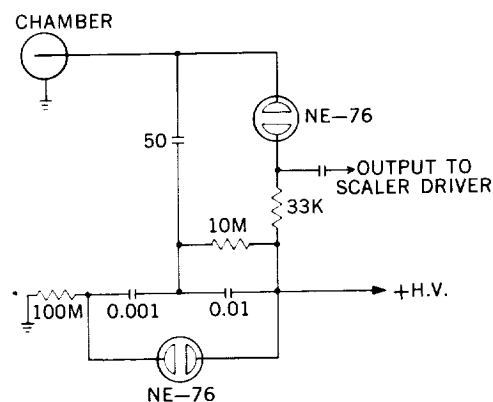


Figure 12 — Converter for measuring low current (Developed by the G. E. Co.)

SIMPLE SUBSYSTEMS

By the use of combinations of slight variations of the basic circuits described above and in Table 2 it is possible to build many subsystems to perform operations at the second level of complexity. To illustrate: a voltage amplitude can be converted from analog to digital form by means of the circuit shown in the block diagram of Figure 13. It can be used as shown for inputs having variations that are slow compared to the clock rate. If the input amplitude variations are more rapid, a pulse lengthener or level clamping circuit can be used to hold the level for the duration of the measurement. Action is initiated by applying a "begin conversion" pulse which opens the clock gate. The scaler counts clock pulses until the staircase level first exceeds the input amplitude. At this point, a comparator output appears which closes the clock gate. The amplitude is then contained in digital form in the scaler and can be commutated, shifted out, or used directly to address a storage matrix.

The pulse height-to-time converter shown in block diagram form in Figure 14 contains a different type of analog-to-digital converter in which a capacitor is initially charged to the input amplitude and a clock gate is opened. The capacitor is permitted to

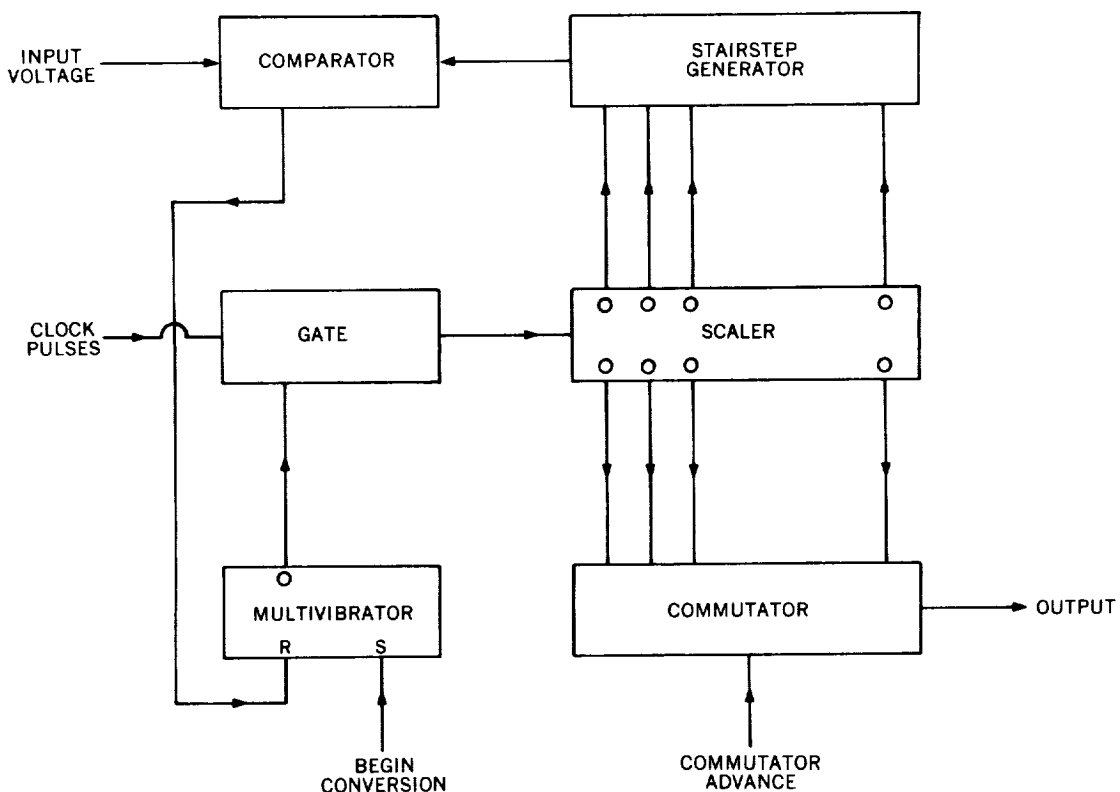


Figure 13 — Stairstep analog-to-digital voltage converter

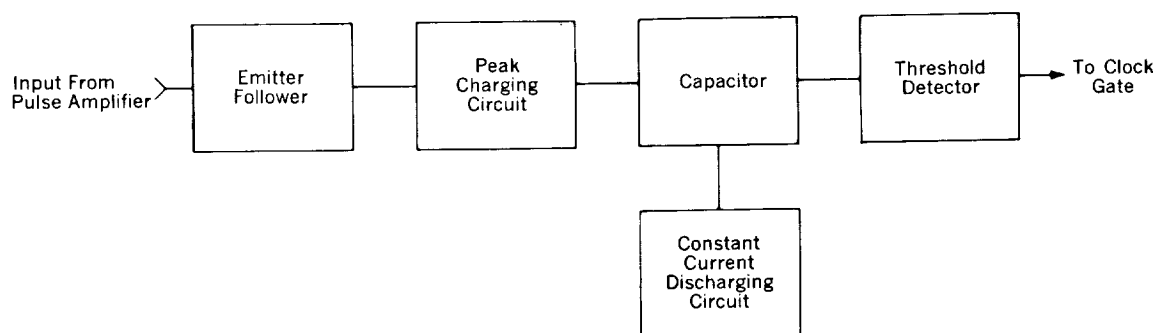


Figure 14 — Ramp pulse-height to time converter

discharge at a constant rate until its voltage reaches a threshold value, at which point the gate is closed. Thus, the gate width is proportional to the input voltage minus the threshold voltage. The gate allows clock pulses to be counted by a scaler, and at the end of the conversion the digital number again resides in the scaler. The conversion speed is about the same as that of the circuit of Figure 13. Both this and the previous circuit can be made with a zero offset by biasing the staircase off-zero in the case of the previous circuit, and by making the threshold voltage non-zero in the latter circuit.

COMPLETE SIGNAL CONDITIONING SYSTEMS

In a spacecraft, the detectors and signal conditioning elements must be assembled in such a manner that meaningful data can be sent to the ground station from a number of detectors, often over a single telemetry system. For example, data from one detector may be accumulated and partially processed while data from another detector are being telemetered. More specifically, the pulse height spectrum from a scintillation counter may be determined and stored in a magnetic core storage matrix while data from a GM counter previously stored in a scaling circuit are being transmitted. Most of the energetic particle detectors can be used in similar time sharing systems. In those cases where full time telemetry is required, the data are either frequency multiplexed or a separate transmitter is used. To illustrate the manner in which data from a number of different detectors are processed, stored, and multiplexed onto a central telemetry link a number of spacecraft systems will be described.

The Explorer I instrumentation is an example of an extremely simple system in which a minimum amount of processing was accomplished before telemetry (References 2 and 9). As can be seen in Figure 15, the information from each sensor directly modulated a subcarrier oscillator, and the subcarrier oscillator outputs were summed in two groups and used to modulate two independent transmitters. The two independently operating systems provided redundancy to increase the reliability.

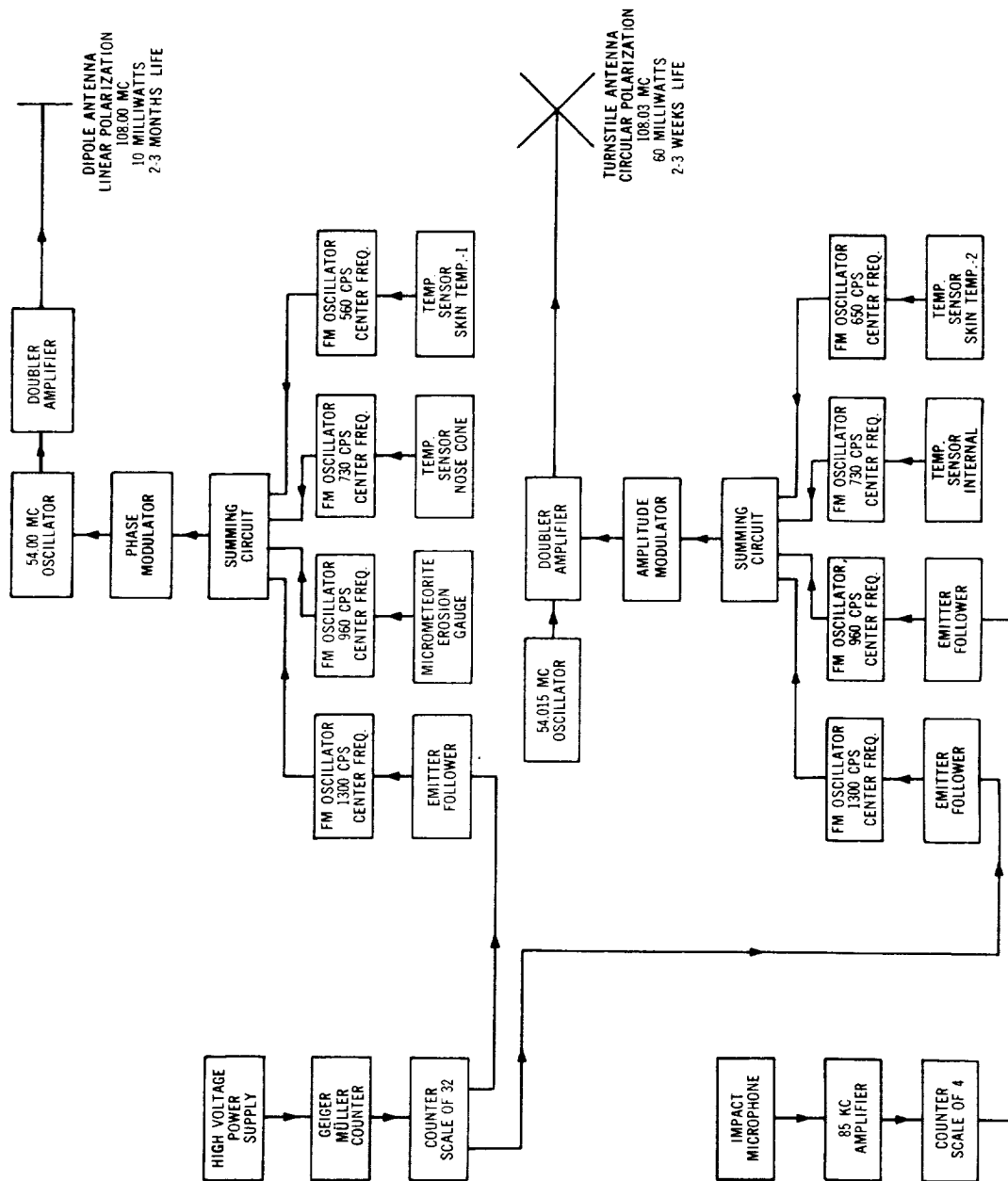


Figure 15 — Explorer I spacecraft data system

The Explorer III system is an example of a satellite data handling system in which very little data processing was employed, but in which tape recorder data storage was provided to allow recovery of information from all positions in the orbit (Reference 10). Figure 16 indicates schematically the manner in which the recorder was used. It should be noted that the tape recorder was made digital in nature, i.e., the tape moved in discontinuous steps, because of the essentially digital nature of the data. This resulted in a low average power requirement for the tape recorder of only 35 milliwatts. The data capacity was 7200 binary bits.

The instrumentation used in Explorer VI (Figure 17), is an example of a somewhat more complex data system (Reference 11). This greater complexity resulted from the larger number of experiments carried and a more advanced telemetry encoding system

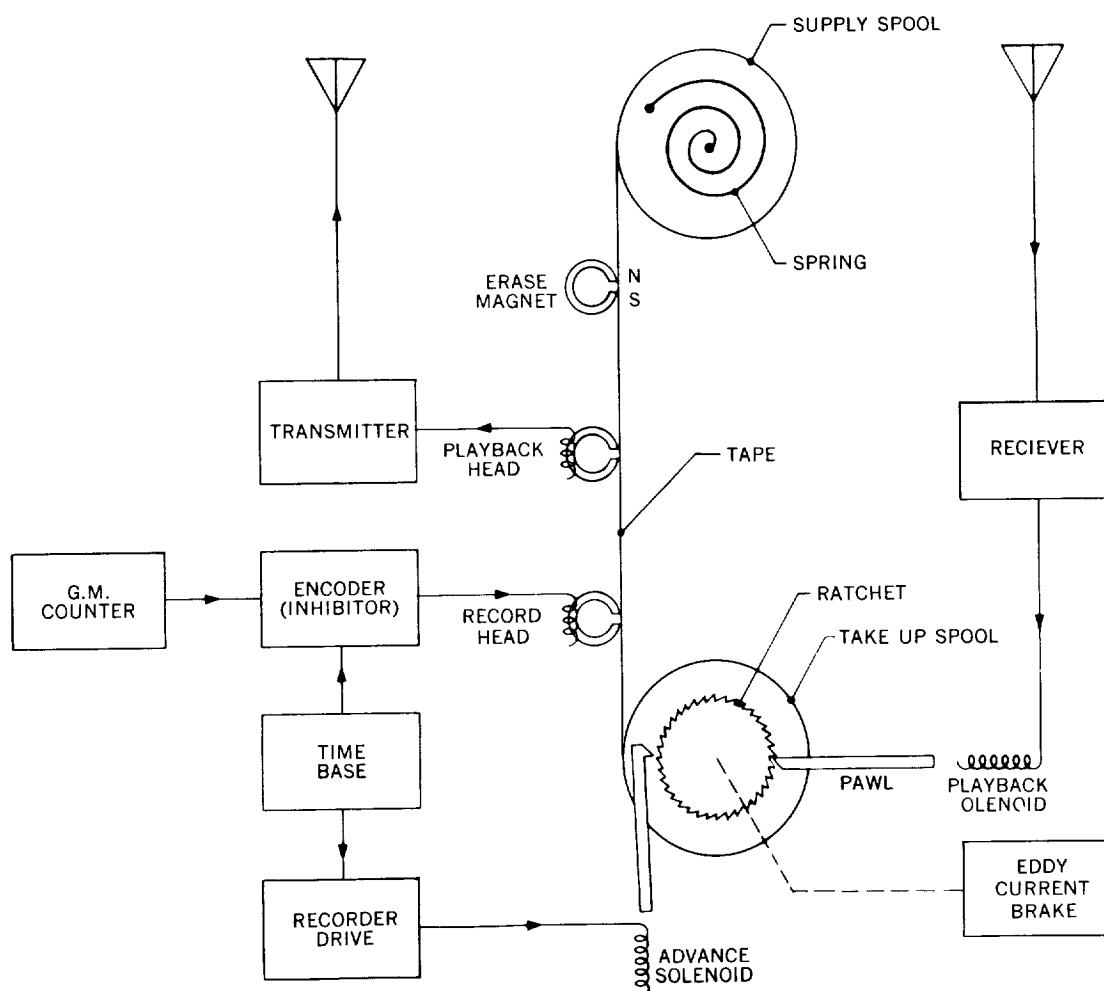


Figure 16 — Simplified diagram of data storage and readout system for Explorer III

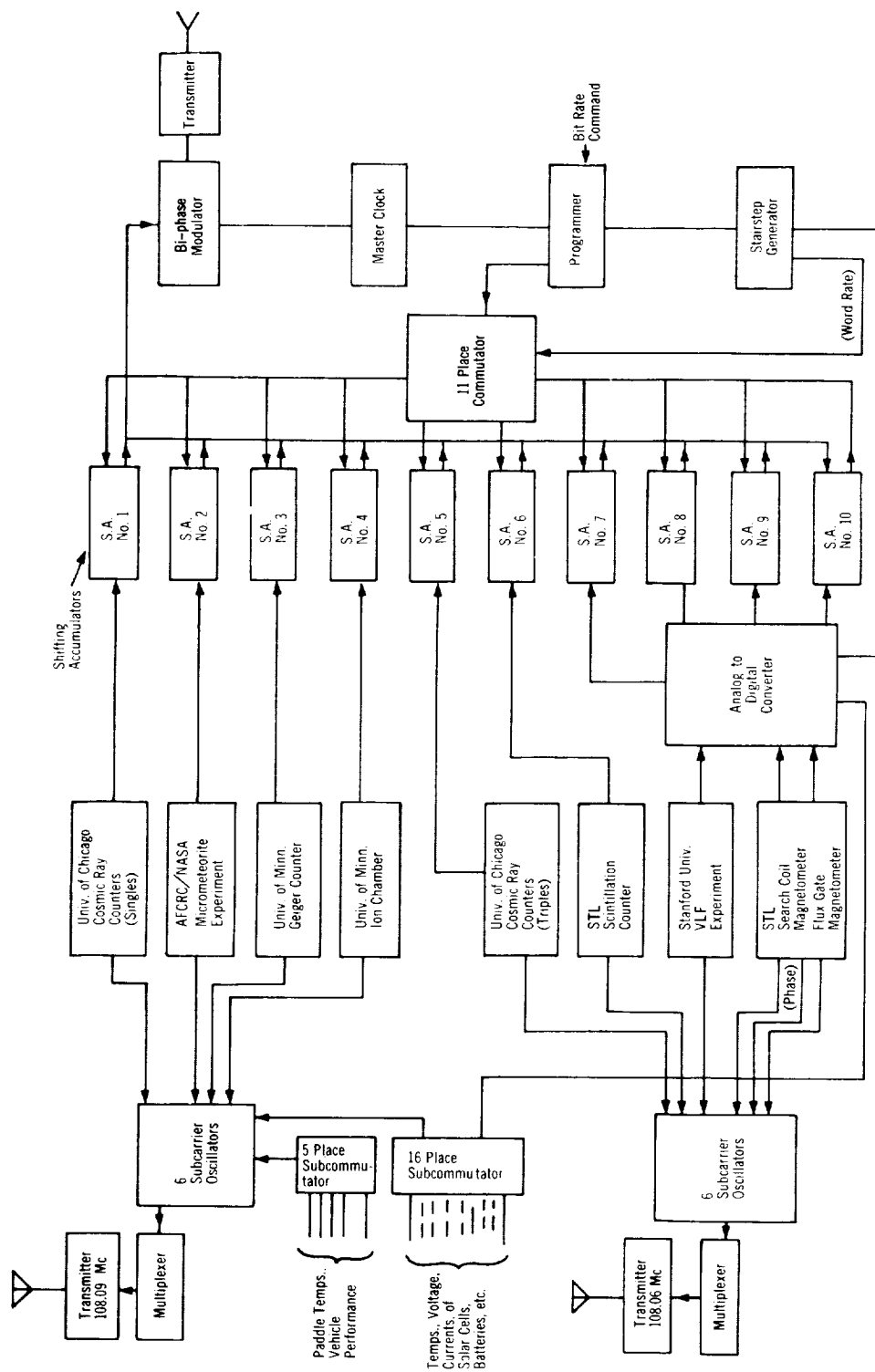


Figure 17 — Telemetry system used in Explorer VI

employed. It should be noted, however, that the amount of data processing before transmission was still small. All the detectors provided outputs to simple preconditioners whose outputs were telemetered. The digital encoding system was a departure from previous practice. An orthogonal code and coherent modulation were employed to decrease the word error probability for low signal-to-noise ratios, as will be described later in this paper. Because this was a new system, a separate telemetry system employing the older frequency multiplexing technique was included as a back-up.

The Explorer XII satellite is an example of a present generation system in which many detectors were employed and in which there was a large amount of data processing before telemetry. Figure 18 is an artists drawing of the complete satellite, which was launched into a highly eccentric orbit (apogee greater than 10 earth radii). The instrumentation was designed to investigate the charged particle energy spectrum from about 100 to more than 10^9 electron volts. Figure 19 indicates the particle fluxes and energy values which were measured. The energetic particles experiments for these investigations were furnished by the NASA Goddard Space Flight Center, the State University of Iowa, and the NASA Ames Research Center. A two-axis flux gate magnetometer was provided by the University of New Hampshire. The satellite structure, power system, telemetry system, thermal control system, despun system, technological experiments, and optical aspect sensor were developed by the Goddard Space Flight Center.

Three of the Goddard Space Flight Center experiments form a major experimental subsystem which will be described to illustrate the more complex data processing techniques employed. These experiments were designed to assist in the study of (1) the cosmic ray accelerating mechanisms, (2) the modulation mechanisms which result in the 11-year variation and the Forbush decreases accompanying certain types of solar activity, and (3) the mechanisms by which solar cosmic rays are produced and modified by solar weather.

This instrumentation is shown in block diagram form in Figure 20. The first detector was a double scintillator telescope which was capable of measuring the proton spectrum in the energy range 70 to 700 Mev. Only particles traversing both elements of the assembly were processed. When a coincidence was obtained, the pulse from one of the scintillator detectors was analyzed by a pulse height analyzer, which sorted the pulses into one of 32 storage channels depending on which of 32 amplitude increments they fell within. The analyzer used the linear pulse amplifier of Figure 10 and a pulse height-to-time converter of the type shown in Figure 14. The gated clock pulses were counted in the address register of a magnetic core storage matrix. At the completion of this operation, one count was added to the number previously stored in the channel addressed by the address register. At the completion of the store mode, the complete pulse height spectrum (differential energy spectrum) was contained within the 16 by 32 core matrix. During the readout mode, these 512 binary bits were sequentially telemetered. The pulse height analyzer described above, designed for use in spacecraft by the Radiation Instrument Development Laboratory, is available

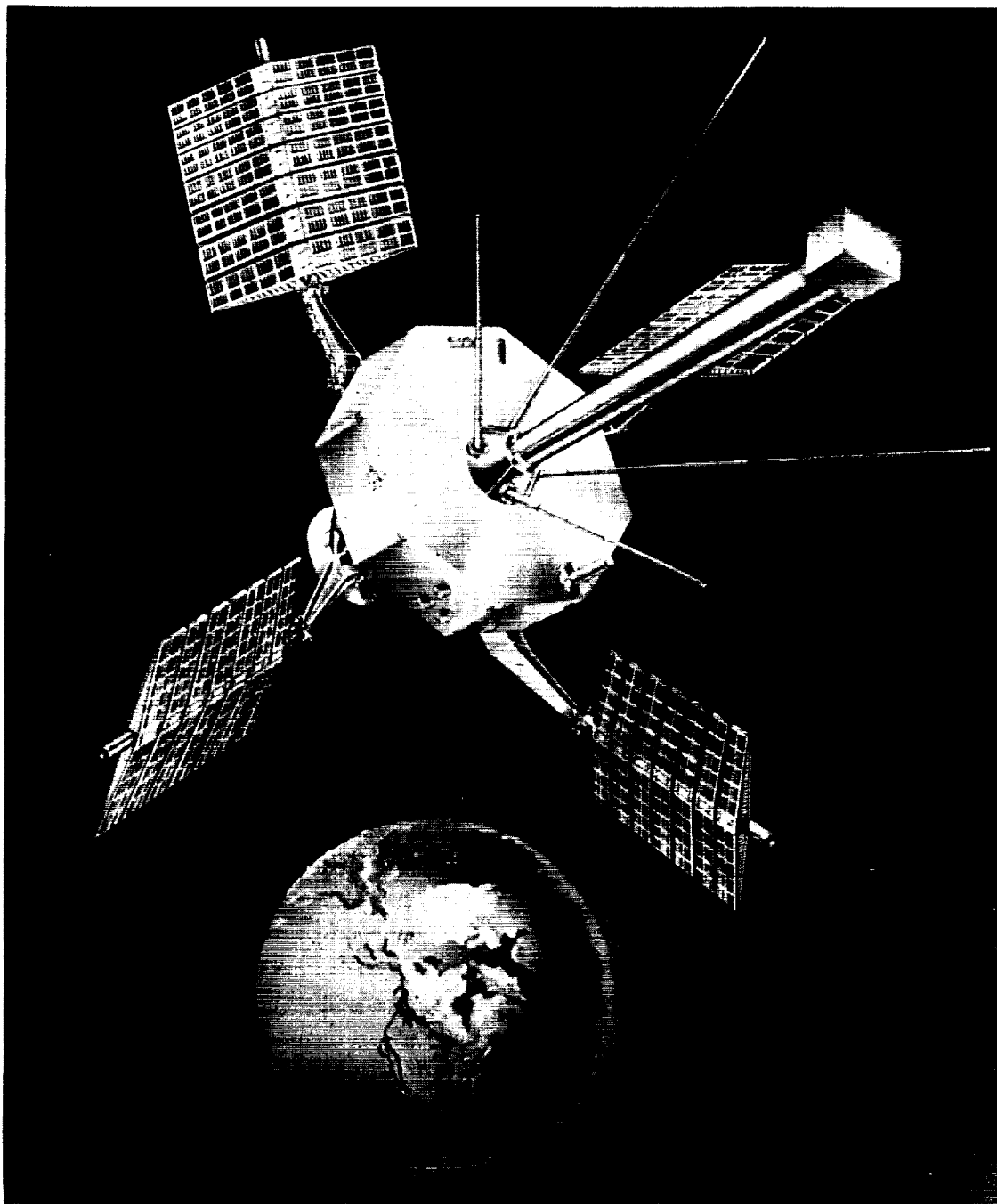


Figure 18 — Artist's drawing of Explorer XII

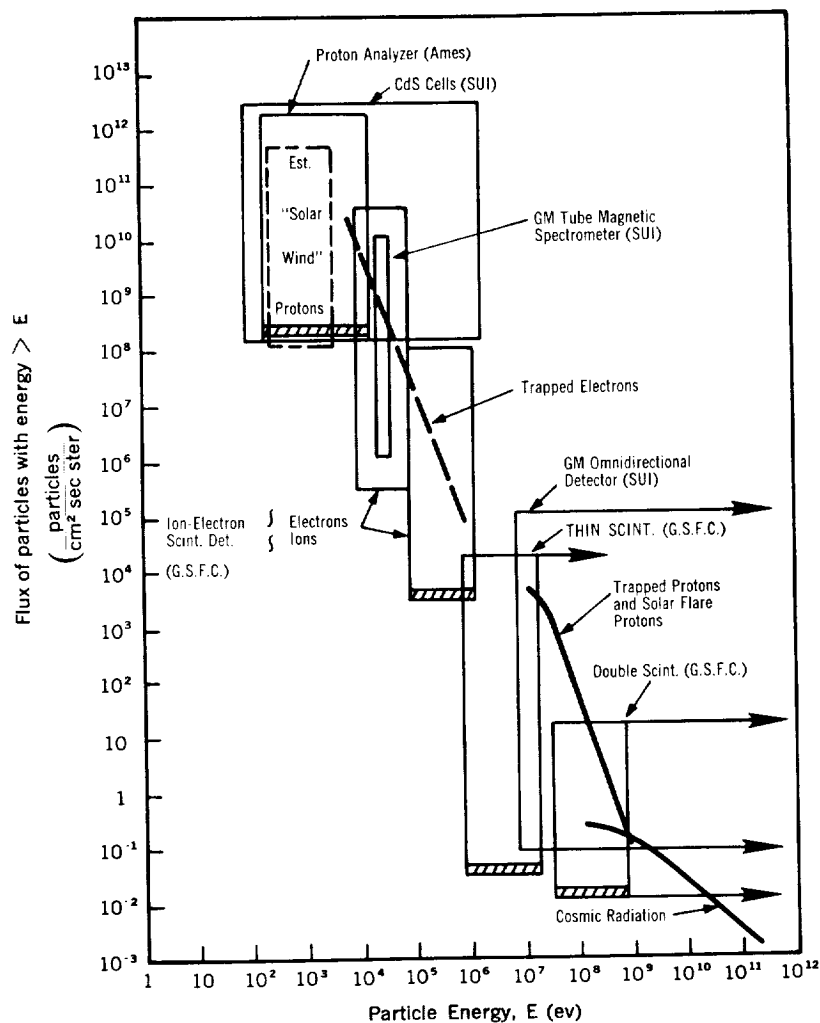


Figure 19 — Ranges of sensitivity for energetic particles measurements on Explorer XII

in a package measuring $15.2 \times 15.2 \times 12.7$ cm, weighing 2.5 kg, and requiring about 1 watt of power.

The second detector, used in this instrumentation to extend the proton energy spectrum down to about 1 Mev, was a thin CsI scintillator detector. The pulse height distribution from this detector was determined by an eight channel integral pulse height analyzer developed at the Goddard Space Flight Center (Reference 6). In this analyzer, a pulse amplitude discriminator level was established by the voltage generated by an eight level stair-step generator. All pulses having amplitudes greater than the discrimination level were counted by a scaler. For each level the pulses were accumulated and then read out. The discriminator was sequentially stepped through its eight levels.

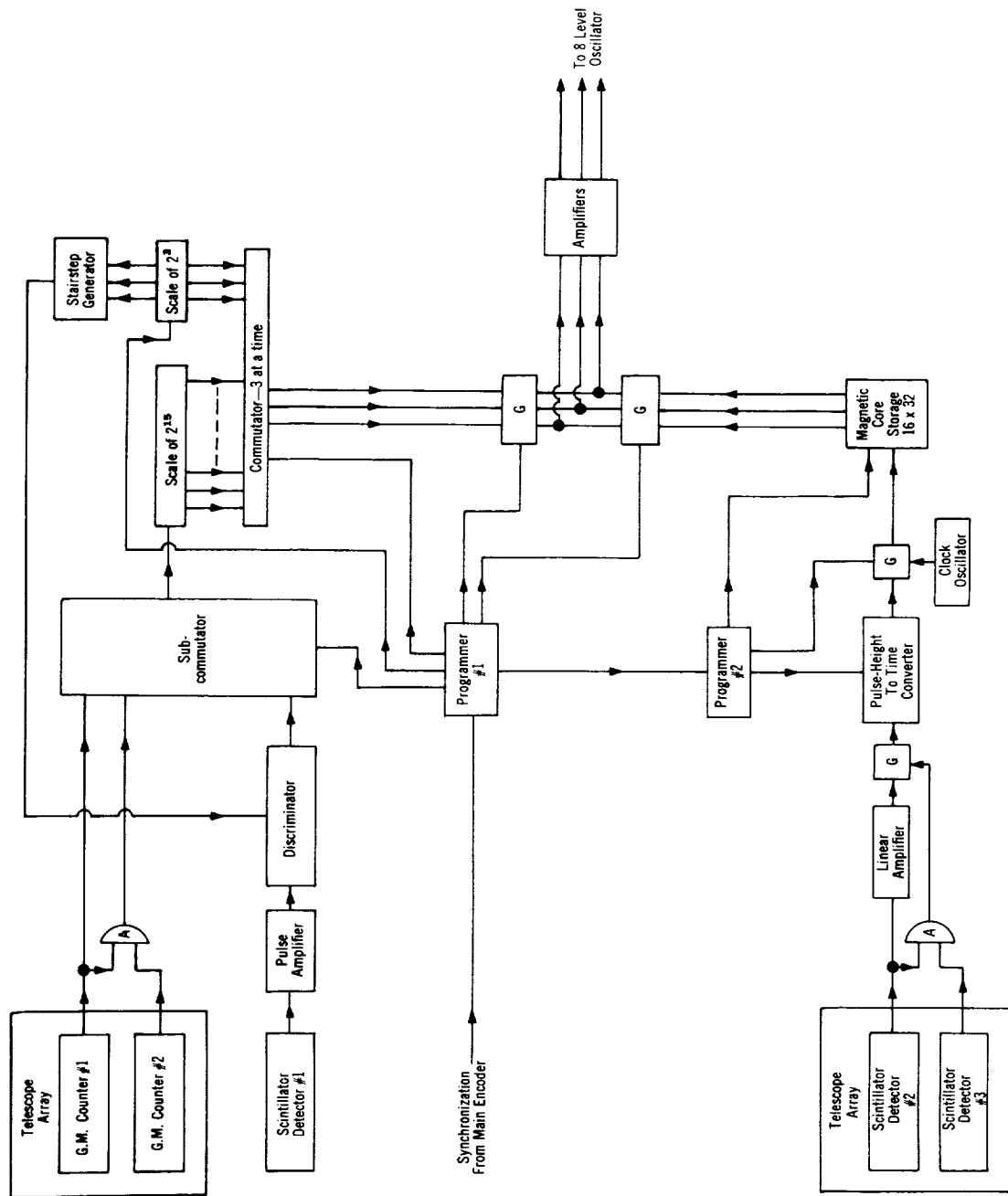


Figure 20 — The Explorer XII cosmic ray experiment signal conditioning system

The third detector employed two Anton type 1003 pancake GM counters arranged to serve as a simple, reliable cosmic ray monitor and to check on the information received from the other two detectors. The counters formed a telescope array, and the coincidence rate and the rate from a single GM counter were accumulated and telemetered sequentially.

A commutating system was included to allow all three detectors to use a common telemetry channel. At the beginning of the commutator cycle the GM counter coincidence events were accumulated for about 1.6 seconds and read into the telemetry system during the following 0.96 second. Then the single GM counter output pulses were accumulated and read for comparable time intervals. The single scintillator detector output pulses, with the discriminator set at the first stairstep level, were accumulated and read during the next 1.6 and 0.96 second periods, respectively. This was repeated for stairstep levels two through eight. Thus, 25.6 seconds were required for reading the counting rates of these two detectors. This sequence was repeated 12 times, requiring a total of slightly more than 5 minutes.

During the time the GM counter and single scintillator detector pulses were being accumulated and read, pulses from the double scintillator telescope were being analyzed and stored in the magnetic core memory. At the completion of this sequence, the data lines to the telemetry system were switched to the analyzer storage system and its read-out began. The stored data were telemetered several times during the ensuing 102 seconds. Thus, a new energy spectrum and a complete set of GM telescope and signal scintillator detector data were obtained every 6.7 minutes.

The subsystem outlined above, including the pulse-height analyzer, was fabricated in the form of five subassemblies using approximately 530 transistors, weighing 5.8 kg, and requiring 1.4 watts of electrical power. One of the circuit boards (subassemblies) used in the construction of the subsystem is shown in Figure 21. This circuit board contains the scaler (of the type shown in Figure 5) used to accumulate the GM tube and single scintillation detector pulses, and the matrix required to read it into telemetry system.

ADVANCED SPACECRAFT CENTRAL DATA HANDLING SYSTEMS

In line with the development of the larger standard observatory spacecraft, such as the Orbiting Geophysical Observatory (OGO) and Mariner, large centralized data handling systems are being developed which can accept the standardized outputs of many sensors and directly associated signal conditioning systems. The OGO data system shown in Figure 22, is an example of this type of advanced system for use in earth satellites where the transmission path length is less than 20 earth radii. This system actually contains three subsystems: a wide-band digital data subsystem, a special purpose analog subsystem, and a radio command subsystem. Since the digital subsystem includes analog-to-digital converters, it will be able to accept a wide variety of digital and analog inputs. The

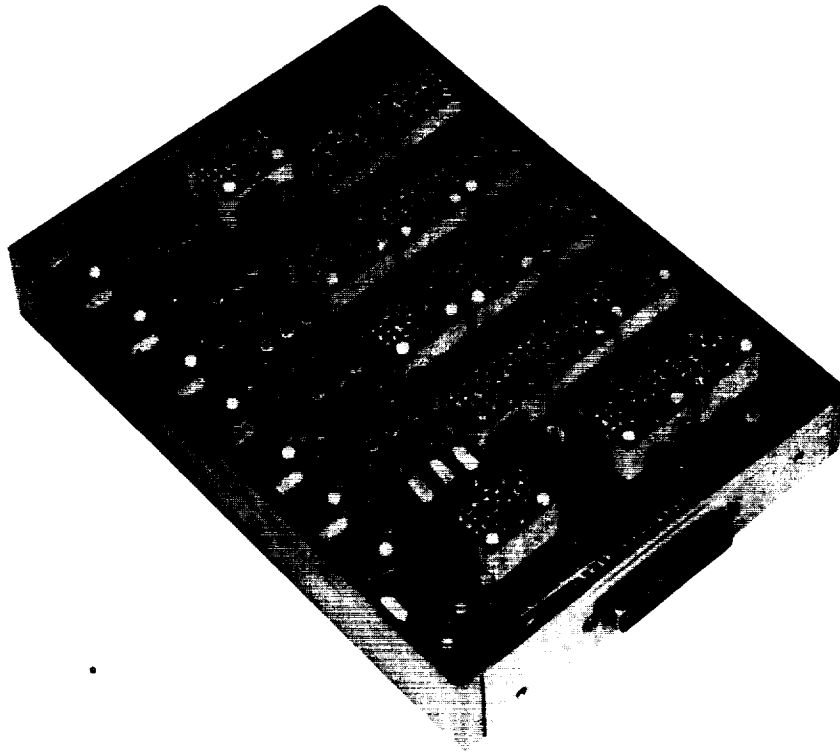


Figure 21 — The Explorer XII cosmic ray experiment logic system accumulator card.
This subassembly is 17.8 cm long.

wide-band subsystem will be capable of telemetering at one of three binary bit rates, 1000, 8000, or 64,000 bits per second, which can be selected by ground command. The digital information will be presented in 9-bit words, with each word representing a data sample, so that about 115, 920, or 7360 words per second can be telemetered. A commutator will be included to allow the sampling of as many as 50 experiments according to a pre-determined format. Thus, on the average, 140 readings per second can be telemetered from each experiment.

The wide-band system also includes a tape recorder storage system capable of storing 85 million binary bits. Continuous storage at a rate of 1000 bits per second is being provided, and readout of the recorder at a high rate by ground command will be possible. Thus, data will be recorded from all positions in the satellite orbit.

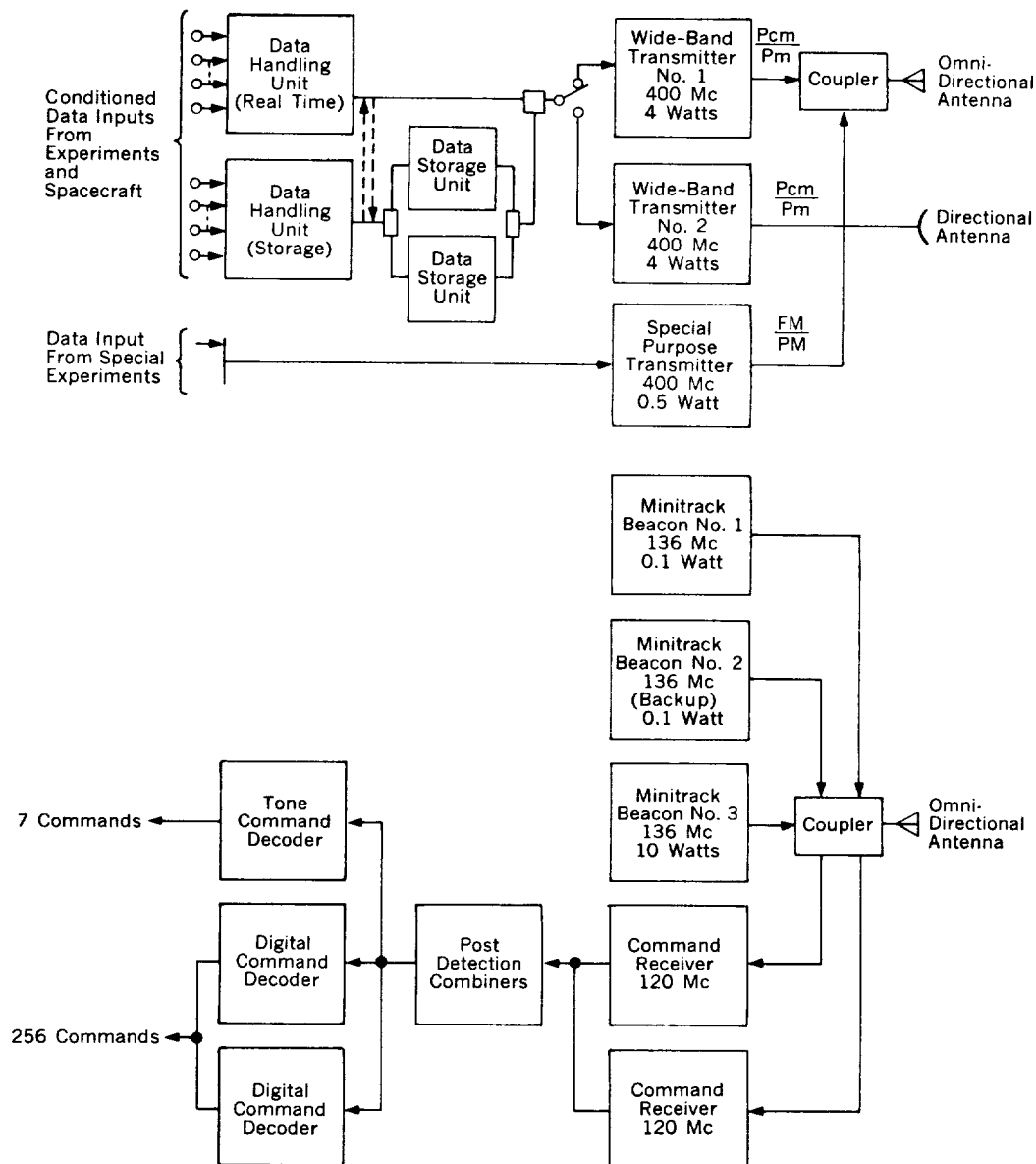


Figure 22 – The Orbiting Geophysical Observatory data and communication system

The special purpose telemetry is being provided for wide-band experiments whose data cannot be digitized easily. The transmitter and antenna system are being provided as a part of the spacecraft, but all signal conditioning instrumentation will be provided by the participating experimenters. The system will have a 200 kc bandwidth.

The command system will be included to permit partial control and fault correction in the spacecraft. Commands will be provided to (1) permit overriding of the stabilization, thermal, and other subsystems, (2) permit control of the data system, (3) turn experiments on and off, and (4) control scaling factors, ranges of operation, etc., in the experiments. A total of about 250 commands will be possible.

In the development of these central spacecraft data handling systems, the goal is to make them as universal as possible and to make the interface between the experimental instrumentation and the data handling systems as simple and well defined as possible. This is expected to reduce the effort required by the experimenters in making instrumentation for many different spacecraft and in making equipment that will work with the data systems properly the first time they are mated.

TELEMETRY

Once the detector signals are processed into a form suitable for transmission, the next problem is that of telemetry. The goal is to obtain as much power per data bit at the ground receiver output per unit transmitter input power as possible, while keeping the noise at the receiver output as low as possible.

The familiar equation for signal-to-noise power ratio is developed as follows (Reference 12): The power area density at a point in space (magnitude of the Poynting vector) is

$$P = \frac{W_t G_t}{4\pi R^2},$$

and the power intercepted by a receiving antenna is

$$W_r = \frac{PA_r}{l}.$$

Thus, the received power is

$$W_r = \frac{W_t G_t A_r}{l 4\pi R^2},$$

where w_t is the transmitted power, G_t is the gain of the transmitting antenna, A_r is the *effective* area of the receiving antenna, R is the distance between transmitting and receiving antennas, and l includes the losses due to polarization misalignment, cabling, etc. Note that the received power is stated in terms of the *gain* of the transmitting antenna and the *effective area* of the receiving antenna. Either the gain or the area of either antenna could be used, since the gain and effective area of any antenna are related by the expression $A_r = G_r \lambda^2 / 4\pi$ where λ is the wavelength.

Table 3 lists the gains and effective areas of several common antennas. The question of whether A_r or G should be used depends only on which is the more significant for a given antenna. An isotropic antenna is defined as having unit gain (for all frequencies) and is therefore most easily characterized by G . A parabolic antenna, on the other hand, is more conveniently characterized by its effective area, since A_r is simply related to its geometric area, while its gain is a function of frequency.

Table 3
Power Gains and Effective Areas of Several Common Antennas

Radiator	Gain Above Isotropic	Effective Area
Isotropic	1	$\lambda^2/4\pi$
Infinitesimal dipole or loop	1.5	$1.5\lambda^2/4\pi$
Half-wave dipole	1.64	$1.64\lambda^2/4\pi$
Parabola (Geometric Area = A)	$(6.3 \text{ to } 7.5) A/\lambda^2$	$(0.5 \text{ to } 0.6) A$
Broadside array (Area = A)	$4\pi A/\lambda^2$ (maximum)	A (maximum)
Turnstile	1.15	$1.15\lambda^2/4\pi$

The selection of an antenna for the ground station depends on a number of factors (Reference 13 and 14). For reception from satellites within several hundred kilometers from the earth, where the initial acquisition must be rapid and the maximum angular rate at the receiving station may exceed 2 degrees per second at the zenith, and for presently used frequencies, the antenna size is limited by mechanical mobility. Present antennas for this purpose located at the stations which make up the Minitrack net are made up of stacked Yagi antennas with total power gains of about 20 db. For spacecraft at distances of more than several earth radii, the limiting factor is a different one. The parabolic antenna is presently capable of giving larger gain for this application than any other type for a given expenditure of effort. But, for the relation between the effective and geometric areas listed in Table 3 to hold, the mechanical surface irregularities of the reflector must not exceed about $\lambda/16$. Thus, as the parabolic antenna is made larger and larger (with constant frequency), a point is reached where a further increase in size will not result in

a proportionate increase in antenna gain unless a large refinement in the precision of antenna construction is made. Figure 23 shows the relation between the antenna power gain and frequency for two parabolic antennas in present use — the 250 foot diameter antenna at Jodrell Bank and the 85 foot diameter antenna at Goldstone Lake, California.

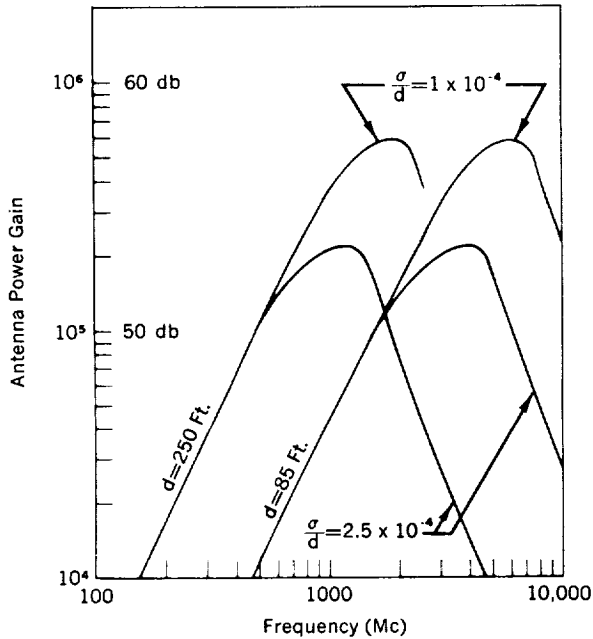


Figure 23 — Antenna power gain vs. frequency for the 85- and 250-foot diameter parabolic antennas. The antenna diameter is d , and σ is the magnitude of the surface irregularities.

The ratio of surface irregularity to diameter $\sigma/d = 10^{-4}$ for the upper curves represents a construction precision of about 3/4 cm for the 250 foot antenna and about 1/4 cm for the 85 foot dish, while the value 2.5×10^{-4} represents precisions of about 2 and 0.6 cm, respectively.

On the spacecraft, the factors limiting antenna size and gain are considerably different. If the spacecraft antenna is not oriented toward the earth, then a radiation pattern approaching isotropic is necessary. Even on stabilized spacecraft, it will not be possible for a number of years to make the antenna as large, as accurate, and as controllable as the earthbound antenna. During the next few years, areas of tens of square meters may be possible; and

later, areas of several thousand square meters may be achieved. But it is expected that the size will always be small compared with that of the earthbound antenna.

The factor l in the expression for the received power represents the losses due to the cabling from the ground antenna to the receiver preamplifier and to misalignment of the planes of polarization of the incident wave and the receiving antenna. The cabling losses can be expected to be several decibels while the loss due to polarization misalignment depends on the type of polarization employed in the two antennas and on their relative alignment. If the spacecraft is stabilized and the polarization plane of the ground antenna can be rotated to correspond with that of the incident wave, then the polarization loss can be virtually eliminated. The power attenuation factor caused by polarization vector misalignment in the general case is (Reference 12):

$$\frac{W}{W_{\max}} = \frac{(1 \pm r_1 r_2)^2 + (r_1 \pm r_2)^2 + (1 - r_1^2)(1 - r_2^2) \cos 2\theta}{2(1 + r_1^2)(1 + r_2^2)},$$

where W_{max} is the power received when the vectors are aligned and rotating in the same direction, r_1 is the axial ratio of the elliptically polarized incident wave, r_2 is the axial ratio of the elliptically polarized receiving antenna, and θ is the angle between the directions of maximum amplitude of the incident wave and antenna; and the positive sign is to be used if the rotational sense is the same for the incident wave and antenna, whereas the minus sign is to be used if they are opposite. Several degenerate cases for this expression are summarized in Table 4. It should be noted that the polarization of the incident wave will, in general, not be the same as that of the transmitted wave, because of atmospheric effects.

The parameter W_t is the power actually radiated by the transmitting antenna, and is less than the total input power to the transmitter by the amount of the cabling losses and the losses due to transmitter inefficiency. At present, it is possible to achieve transmitting system efficiencies between 30 and 80 percent for transmitters below 1000 Mc, and on the order of 10 to 50 percent above 1000 Mc; these figures are not likely to be improved appreciably. In computing the received *information* power, it is necessary that the *usable sideband* power rather than the total radiated power be used. But in computing the received power for *tracking* purposes, where only the carrier power is employed, only the radiated carrier power must be used. If the same transmitting system is to be used for both tracking and data transmission, then a ratio of carrier to usable sideband power should be selected which will result in comparable reception thresholds for the two signals. This ratio can be optimized by a proper choice of modulation method and modulation index.

Table 4

Polarization Losses for Linear and Circular Polarization

Polarization of Incident Wave	Polarization of Receiving Antenna	Sense of Rotation	$\frac{W}{W_{max}}$
Circular	Circular	Similar	1
Circular	Circular	Opposite	0
Circular	Linear	-----	1/2
Linear	Circular	-----	1/2
Linear	Linear	-----	$\cos^2 \theta$

If there were no interference, any transmitter signal could be received from any distance by incorporating sufficient amplification in the receiver. Interference, however, always limits the usable range of communication (References 13, 14, and 15). It enters at every point in the telemetry link. In the transmitter, it is caused by the instability of the oscillator. In the transmitter-receiver space link, it enters from galactic, solar, planetary, and atmospheric sources. And in the receiver circuits, interference is generated by the random motion of electrons and by oscillator instabilities of the type that occur in the transmitter. Every effort is made to reduce the effect of these interfering sources in order to produce as high a ratio of received signal power to total interference power as possible. For most spacecraft data systems the interference produced by oscillators, both in the transmitter and receiver, can be made much smaller than that from other sources. The remaining interference is of two types, external and thermal. The external noise includes mostly man-made noise, which is reduced by locating the receiving stations as far from civilization as possible, by careful design of the antenna, and by proper choice of distinctive coding methods to allow reading the data through the noise.

The thermal noise, due primarily to the random motion of electrons, imposes a fundamental limitation. The noise power produced by a thermal source is

$$W_{NT} = kTB,$$

where W_{NT} is the noise power, k is the Boltzman's constant $= 1.38 \times 10^{-23}$ w-sec/°K, T is the absolute temperature in °K, and B is the bandwidth in cps.

There are two obvious ways of minimizing the noise power: by reducing either T or B . Since the reduction of B implies reduction of the telemetered information rate, every attempt should be made to make T as low as possible. The temperature T is the temperature of the equivalent resistor which represents a noise source. It also has a significant relationship to the equivalent temperature of those portions of earth, atmosphere, planets, sun, and galaxy which are seen by the receiving antenna. The value of T to be used in the equation is the properly weighted sum of all the source temperatures, where the weighting depends on how the source is "seen" by the receiving system. For sources which are internal to the receiving system or uniformly surround the antenna, the weighting factor is unity. For sources which occupy only a fraction of the antenna pattern, the weighting factor depends on the size of the source and where within the antenna pattern it is located. The weighted temperature T_{nw} for a source n is given by

$$T_{nw} = \frac{1}{4\pi} \iint T_n(\phi, \theta) G(\phi, \theta) d\phi d\theta ,$$

where T_n is the equivalent temperature of source n , G is the antenna gain, and ϕ and θ are angular coordinates, measured with respect to the central antenna beam axis.

The temperature T , then, is simply

$$T = \sum_n T_{nw}.$$

Typical values of T_n for the various sources are as follows:

1. *Receiver noise.* The equivalent noise temperatures for conventional, parametric-amplifier, and maser receivers are 2000, 100, and 10 °K respectively.

2. *Earth blackbody radiation.* If the antenna "sees" the earth within a portion of its radiation pattern, then noise due to the blackbody radiation of the earth at a temperature of about 280 °K is received. This source is essentially frequency-independent. Antennas whose sidelobe levels are low and which accept very little of this noise are called low-temperature antennas. They are characterized by equivalent temperatures of from 10 to 20 °K. A more conventional well-made parabola and feed may have a temperature of about 100 °K.

3. *Atmospheric noise.* The atmospheric noise is a strong function of frequency and of path length through the atmosphere (Figure 24). For angles above the horizon greater than 10 degrees, the equivalent noise temperature is less than about 10 °K. It can be seen that the performance of good maser systems will be seriously degraded at elevation angles below 10 degrees because of the atmospheric noise and because the antenna sidelobes will intercept the earth. The consequences are not serious for deep space communication where the elevation angle can be kept greater than 10 degrees, but may be for low altitude satellites which spend proportionately more time below this elevation angle.

4. *Galactic (cosmic) noise.* The galactic noise is a strong function of frequency and of the viewing direction, as is shown in Figures 24 and 25. At 270 degrees celestial longitude in the plane of the ecliptic, the direction is very nearly toward the galactic center, and a high temperature results from the integrated effect of the large number of discrete sources seen. The small peak at 90 degrees is the other interception of the galactic and ecliptic planes. For other directions, the noise temperatures for receiver frequencies of 100 and 250 Mc are about 500 and 30 °K respectively.

5. *Radio star, solar, lunar, and planetary noise.* In addition to the diffuse galactic source discussed above, there are a number of discrete sources, generally less than a degree in extent. Included are radio stars, which may not necessarily be identified with visible objects; the sun; the moon; and the other planets. In speaking of these sources, which occupy a very small portion of the antenna beam, it is customary to talk of their

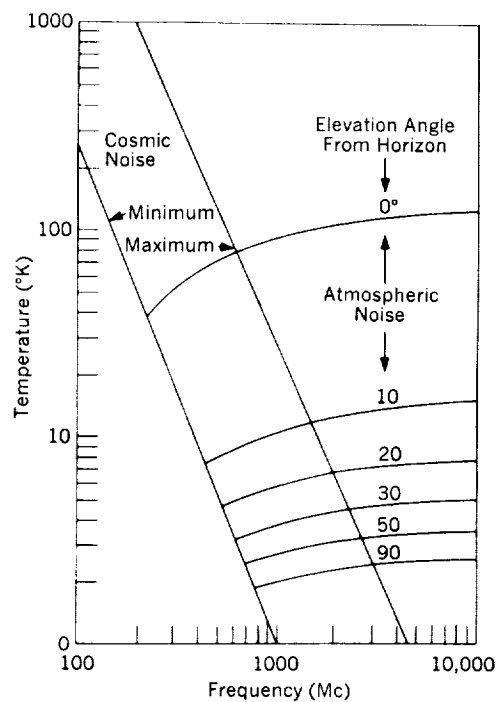


Figure 24 — Atmospheric and cosmic noise as a function of frequency

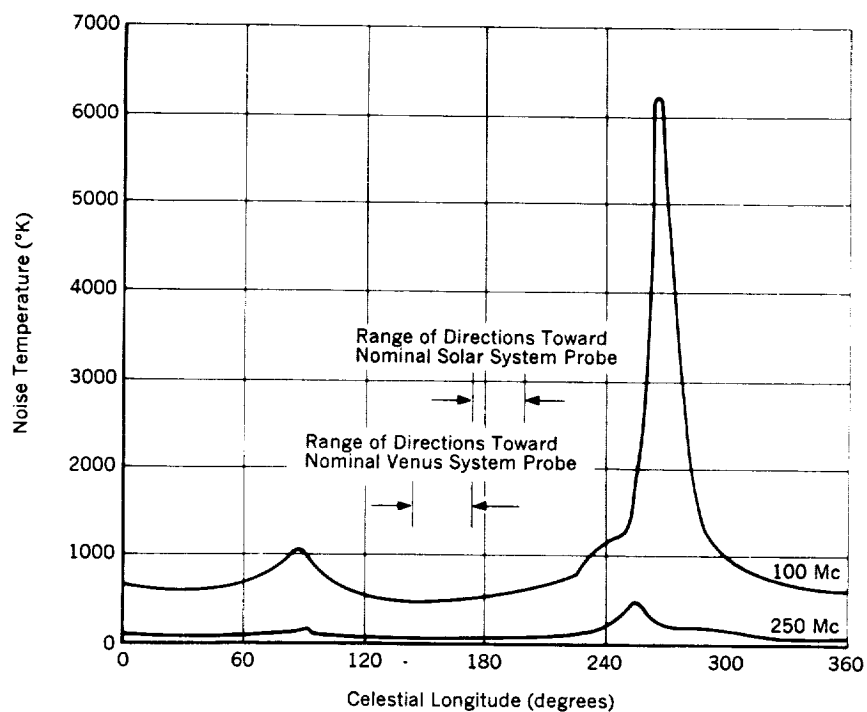


Figure 25 — Galactic radio noise temperature in the plane of the ecliptic as a function of longitude. Longitude is measured east from the vernal equinox.

energy flux-density S at the position of the earth rather than T . The relationships are described by

$$T = \frac{\lambda^2 S}{8\pi k} ,$$

and

$$W_{ND} = SA_e B ,$$

where W_{ND} is the noise power from a discrete source, A_e is the effective antenna area, and B is the bandwidth, as before.

The most intense radio star known is Cassiopeia A. At a frequency of 20 Mc, it produces a flux density of 5×10^{-22} w/m²-cps. The flux density decreases with increasing frequency, reaching values of 2×10^{-22} and 6×10^{-24} w/m²-cps at 100 Mc and 10,000 Mc, respectively. The next most intense source produces only about half as much flux density as Cassiopeia A, and only four of the remaining ones reach 10^{-23} w/m²-cps. For antenna diameters of less than about 100 feet, the noise power received from a radio star will be less than that received from a rather weak galactic region.

The solar electromagnetic radiation is both complex and variable, as Figure 26 shows. It consists of thermal radiation at a blackbody temperature of 6000 °K on which additional noise due to solar activity is superimposed. Thus, it can be seen that the sun is a very intense source, and takes on secondary importance in most cases only because it is localized.

The moon and planets may be disregarded as noise sources for most practical considerations. Some of the planets are sources of noise bursts at certain frequencies which can be avoided. The thermal noise flux density for the moon has been shown to be about 10^{-21} w/m²-cps at a frequency of 35,000 Mc, but is presumably immeasurably small at frequencies below the microwave region. Of the planets, Venus has the highest thermal flux of 10^{-24} w/m²-cps at 9500 Mc. As in the case of the moon, the planetary thermal fluxes are measurable only at microwave frequencies.

The remaining parameter affecting the amount of noise power in the receiver output is the bandwidth. Both the predetection and the postdetection bandwidths must be considered. They are approximately equal to the smallest bandwidths encountered in the circuits ahead of and following the detector, respectively, as long as most noise is introduced ahead of these circuits and all circuits are operated linearly. The value of B to be used in the above noise computation is approximately equal to the smaller of these two figures. Obviously B should be the smallest value which will still pass the desired information. The relationship between B and H , the information bit rate, depends on the type of modulation and detection employed.

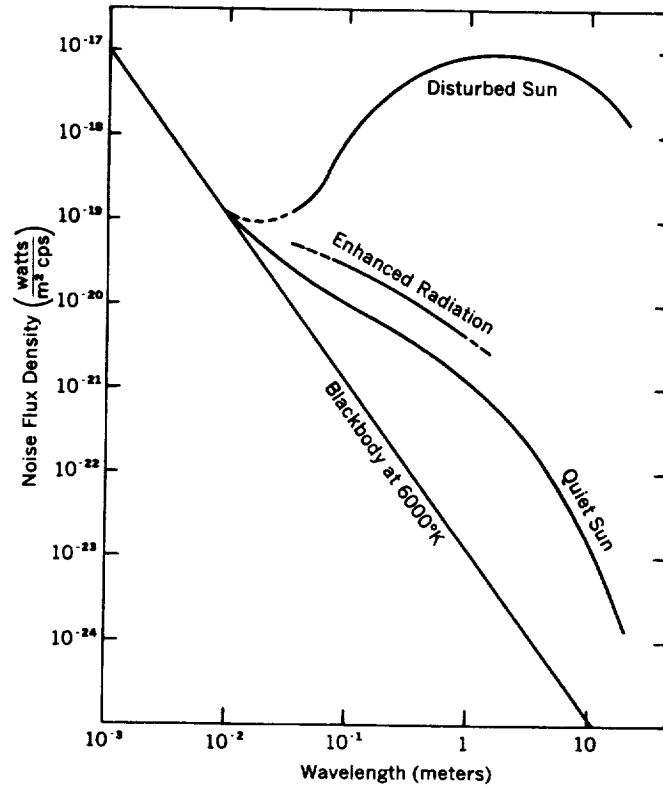


Figure 26 — Representative solar noise levels as a function of wavelength

It is now possible to write the complete expression for the signal-to-noise power ratio at the output of the receiver:

$$\frac{W_r}{W_N} = \left(\frac{S}{N} \right)_P = \frac{W_t G_t A_r}{4R^2 kTB}$$

where all the parameters have been discussed above. A threshold signal-to-noise ratio is usually defined as $(S/N)_T = 1$. Usable data have been received when $(S/N)_P$ has been as low as several db. It is usually true that $(S/N)_P = 10$ db is considered marginal and $(S/N)_P = 15$ db is desirable when machine data reduction systems are used. In order to produce a better comprehension of the numbers involved, the relationships among the various parameters for several sample spacecraft systems are shown in Table 5.

Table 5
Representative Telemetry System Performance

Spacecraft	W_t (watts)	Transmitter Antenna Gain	Receiver Antenna Gain	λ (m)	R (km)	B (cps)	$\left(\frac{S}{N}\right)_P$ (db)
Explorer I	0.01	1.64	50	2.78	4.8×10^3	20	3
OGO*	5	16.00	10^4	0.75	9.6×10^4	2×10^5	15
Pioneer V	5	1.15	2×10^5	0.31	3.2×10^7	10	3

*Orbiting Geophysical Observatory

ENCODING AND DETECTION

The expression given above for the signal-to-noise power ratio is true for systems using any modulation technique, as long as the values of the various parameters are the same. This is not, however, a true index of telemetry system performance, since the experimenter is really interested in the ratio of the amount of information transmitted per unit time to the total transmitter input power. Several factors in addition to the ones discussed above cause systems to give different performances. The first is the relationship between the information and receiver bandwidths. It is customary to express this in terms of the parameter $\alpha = B/H$, where B is the receiver bandwidth as before, and H is the information rate in bits per second. The bandwidth should be made just large enough to permit recovery of the information. The second factor is the ratio of the usable radiated side-band power to the total transmitter power output.

A comparison of the various encoding methods usually results in the conclusion that the most efficient one for space telemetry is pulse code modulation (Reference 16). This is modulation in which a pulse amplitude, phase, or frequency sequentially assumes one of a number L of discrete values. In many cases this will be simple binary code (off-on or phase reversal) modulation in which $L = 2$. Alternatively, a code can be made up of L words, each one consisting of a number M of binary bits. If $2^M > L$, then redundancy is introduced and techniques can be used which result in relatively low error probabilities for low values of S/N. The moderate complexity introduced by the use of these codes is warranted in the case of small satellites, deepspace probes, and planetary spacecraft, on which it is difficult to achieve usable information rates by the more conventional techniques. A particularly interesting code, known as an orthogonal code, is one for which $L = M$, and in which the incoming word is correlated simultaneously with all L possible words (Reference 17). There are L correlator outputs, on which appear zeros for the

wrong possibilities and A for the correct one (under noise-free conditions). A decision device selects the line having the greatest output. In the event that noise is present, so that one digital bit in the incoming word is incorrect, there will still be a high probability for selecting the proper word because of the redundancy. This decision process is known as maximum-likelihood detection, and can be shown to minimize the probability of error when all the words are equally likely and contain equal energies.

The carrier detection method must be carefully selected. It has already been stated that all receiver circuits including the detector should be linear, especially at low signal levels. A commonly used linear detection method is cross-correlation detection (Reference 18) in which the incoming signal plus noise ($S + N$) is multiplied by a locally generated best estimate of signal S^* :

$$S*(S + N) = SS^* + NS^* ,$$

which, when averaged by a low-pass filter, yields the correlation coefficient $(SS^*)_{ave}$ contaminated by the noise $(NS^*)_{ave}$. This process is linear in that the output signal-to-noise ratio SS^*/NS^* is the same as that at the input. By comparison, in conventional square law detection the detector output at low signal levels is

$$(S + N)^2 = S^2 + N^2 + 2SN .$$

In this process, the output signal-to-noise ratio is

$$\frac{S^2}{N^2 + 2SN} = \frac{S}{N} \frac{1}{\left(2 + \frac{N}{S}\right)} .$$

Thus, the degradation of signal-to-noise ratio for square-law detection compared with correlation detection is $2 + (N/S)$. A practical method of constructing a correlation detector is by the use of a phase-locked loop receiver.

Related to the problem of detection is one of signal coherence. A coherent system is one in which the receiver is assumed to know at all times the phase of the unmodulated transmitted signal. The *a priori* knowledge of the signal characteristic is greater for a coherent signal than for a noncoherent signal; thus, some advantage may be expected if the detection system is designed to take advantage of this knowledge. An example of a coherent system is one employing bi-phase carrier modulation, in which the carrier wave phases are 180 degrees apart for binary 0's and 1's.

DATA RECOVERY

It is necessary to perform numerous functions at the stations where the spacecraft data are received. As Figure 27 shows, these may include:

1. *Data recovery.* Receivers and primary data recorders for the receipt of the spacecraft data are necessary.

2. *Spacecraft command.* In many cases the spacecraft contains a command system, which may be used to (a) control the transmitters, recorders, and other elements of the spacecraft data system; (b) control other spacecraft subsystems such as the stabilization system (for example, to direct a telescope at a new star), the power system, or the thermal control system; or (c) control experiments by turning their power off or on, change scale factors, change viewing directions, etc. Some receiving stations have transmitters and code generators to supply the necessary command signals. These commands may be transmitted according to a predetermined plan or upon looking at a live or delayed data display.

3. *Tracking.* Stations which are established to receive spacecraft data usually have tracking systems as well. This tracking function may use parts of the telemetry receiver and antenna, as in the case of the Goldstone Lake station, or it may be provided by a different antenna and receiver system, as in the case of the Minitrack interferometer tracking system.

4. *Timing.* Since it is necessary that specific experimental data be associated with position in space, it is necessary that accurate time be recorded with the received data. The use of a spacecraft clock will not obviate this need, since it will still be necessary to determine the spacecraft clock error by comparison with an accurate clock on the ground. The usual technique is to provide a stable, precise oscillator at the receiving station which is continuously or periodically compared with one of the standard time facilities such as radio station WWV. This local time signal is recorded on the magnetic tape along with the received spacecraft signals.

5. *Real-time Display.* For some spacecraft, it will be necessary to reduce certain portions of the data in real time at some of the receiving stations (and perhaps ultimately at the operations control center by means of microwave or wire communications) so that immediate corrective action may be taken in the event of a spacecraft subsystem malfunction or of a need to readjust an experiment. Little real-time display has been necessary so far, but, with the coming of the observatory-type spacecraft, the need is rapidly developing for some real-time display at least at one central receiving station.

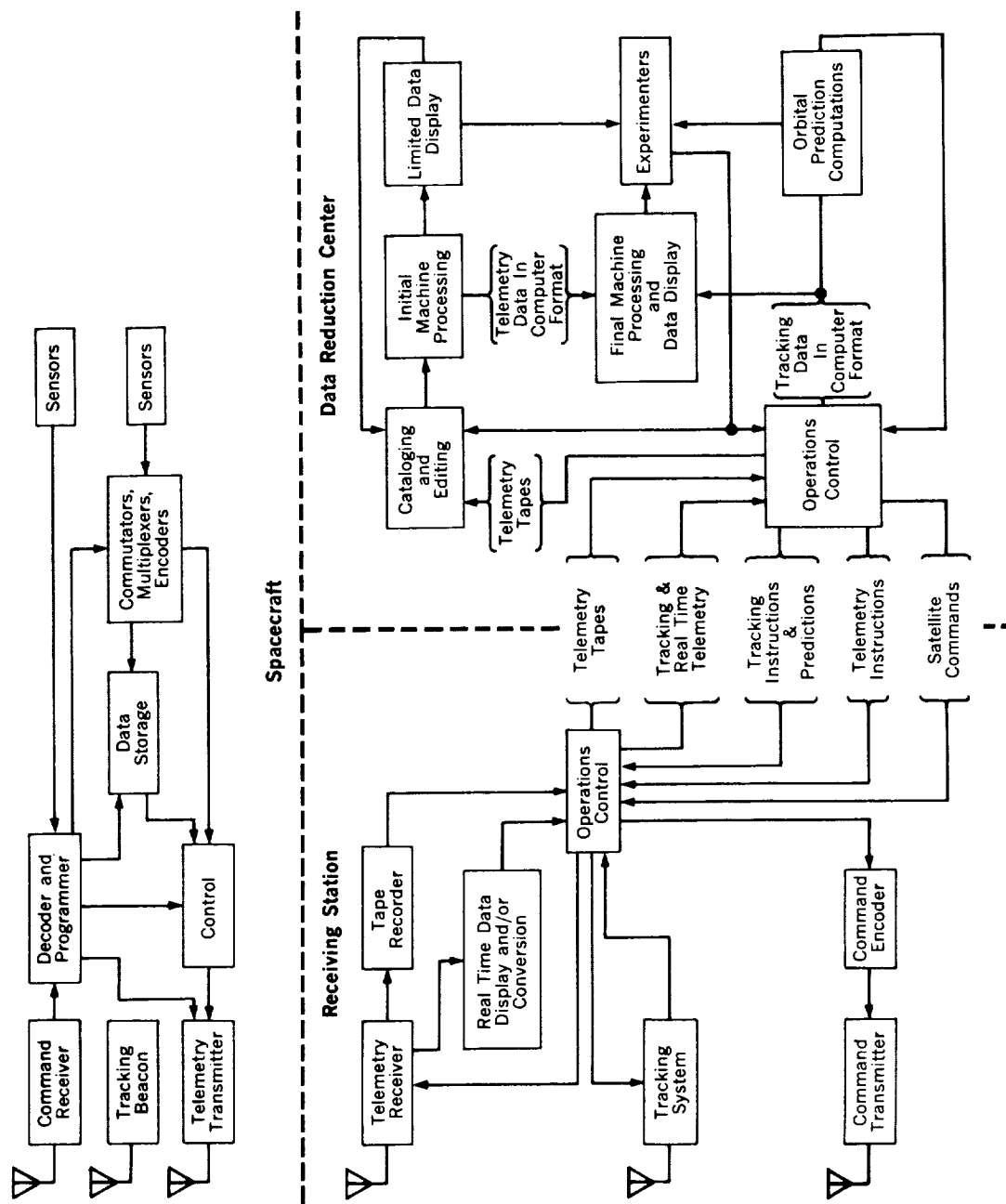


Figure 27 — Information flow in a spacecraft data and communications system

DATA REDUCTION

Once the telemetry receiver output is available on the magnetic tapes it is necessary to reduce these electrical signals into usable data. The magnitude of this task should not be underestimated. The number of data points received from a single satellite can be extremely large. From the single GM counter flown in Explorer I (about the simplest spacecraft data system conceivable, but where essentially no processing was done before transmission) roughly 100,000 data points were received during the active satellite lifetime of 32 days (a data point is a number obtained from a detector which can be associated with satellite position, time, measuring interval, etc.). Other more complex systems have already yielded hundreds of thousands of data points, and the OGO spacecraft will be capable of providing 2×10^{11} data points during its lifetime. Obviously the establishment of techniques for handling this volume of data cannot be assigned a low priority, to be taken care of after the launching is successful. Also obviously, the time proven techniques for reading data "by hand" are not adequate for reducing spacecraft data, except for "quick look" investigations.

The usual procedure for the handling of the telemetry tapes is shown in Figure 27. They are forwarded to a central data reducing center at one of the NASA research centers or, under certain circumstances, directly to an experimenter's laboratory. There they are partially reduced, and the results are recorded on a medium which can be directly used by the experimenters. These reduced data may take several forms including computer tapes or cards, other magnetic tapes, oscillograms, or tabulations. The experimenters then further process these data so that they can conduct their analysis most conveniently.

The use of high-speed computers for initial reduction of receiver output tapes and for final reduction by experimenters is becoming more and more necessary. Both of the two main data reduction steps — the separation of the signals from the noise, and the processing of the "clean" signals — can be accomplished by properly programmed general purpose computers or by properly designed special purpose computers.

A very simple data reduction system (Figure 28) was used in the early Explorer IV reduction program. The discriminators and moving pen oscillograph produced a paper chart which was read by trained data readers. The manual operations required the expenditure of approximately 6 man-years of effort to complete the reduction of about 6 weeks' data. Subsequently, a machine reduction system was perfected which produced IBM punched cards in a single operation. This method proved considerably more accurate than the manual method.

A representative present generation data reduction system is the Explorer VIII system (Figure 29). A similar system will be used for the Explorer XII and S-51 (U.K.) spacecraft. These spacecraft all make use of tone burst modulation, in which an audio

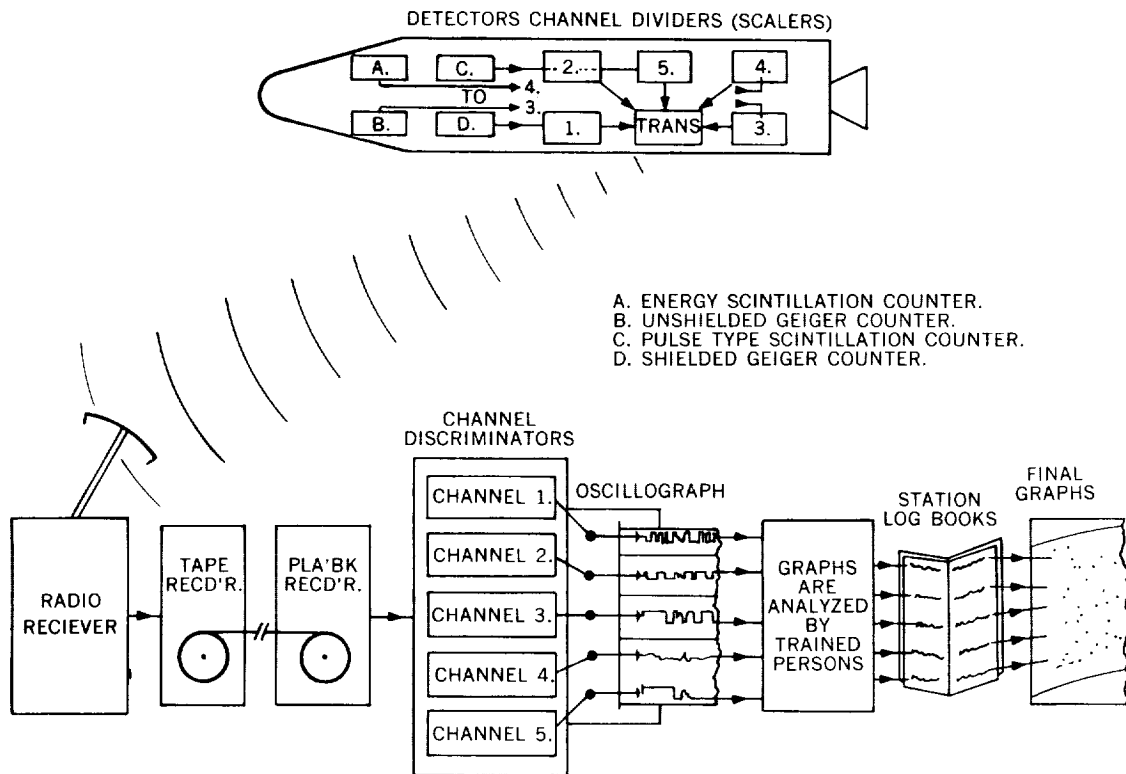


Figure 28 — The Explorer IV manual data reduction process

frequency (5 to 15 kc) oscillator is gated on and off. In the Explorer XII and S-51 systems, the oscillator tone bursts of 10 milliseconds duration are followed by 10 millisecond pauses. The frequency of the oscillator during the bursts is controlled by the data. A single burst frequency can telemeter n digital bits, in which case there will be 2^n possible discrete frequencies. Alternatively, the burst can send analog data by making the frequency proportional to the signal amplitude. The data system includes a commutator, so that one burst is used for experiment 1, another for experiment 2, and so on. In Explorer XII, the commutator had 16 inputs so that each frame was 16 bursts long. Frame synchronization was provided by making the first burst in each frame longer than the others.

In the data reduction process, the magnetic tape recorder output is fed through a 120-tooth comb filter, from which there are 120 output lines. The burst quantizer establishes the burst and frame synchronization. The frequency quantizer integrates the outputs of the 120 lines during the time that the bursts are present, and selects the one having the greatest output amplitude. The quantizer outputs are fed to the decommutator, which reassembles the original data words. These words, plus the time signal, are recorded in computer format on a magnetic tape; this may be used for further data reduction,

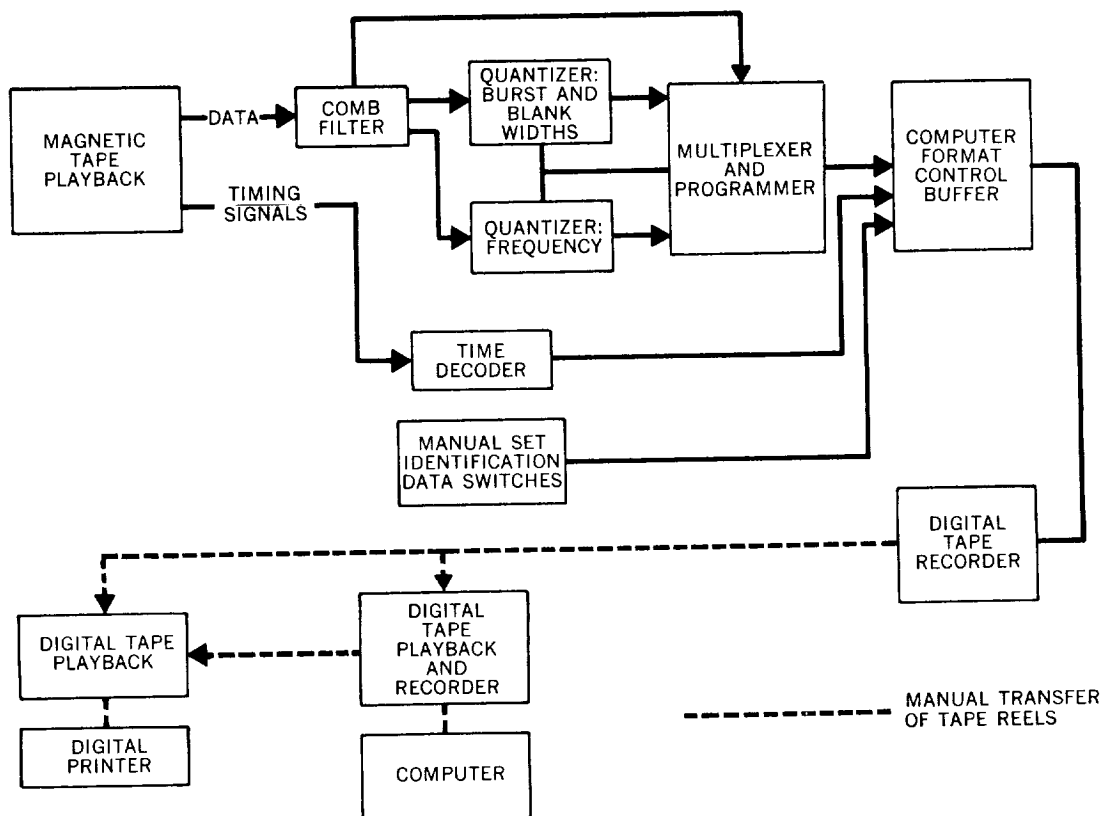


Figure 29 — The Explorer VIII data processing system

tabulation, or display by the computer, either at the central data reduction facility or by the experimenter.

CONCLUDING REMARKS

This paper has discussed a few of the problems involved in properly designing a spacecraft data handling system, including the initial conditioning of the signals from the spacecraft sensors, the transmission of these conditioned signals to the earth, and the processing of the data after receipt. Although it is not necessary that the experimenter understand all the details of many parts of the system, he should have a general understanding of the problems involved so that he can make the most efficient use of the spacecraft. He must be particularly familiar with many of the processes occurring at the two ends of the system (i.e., immediately following the spacecraft sensors, and just before the data appear in final form at the output of the ground data reduction equipment), since these are the places in the system where the basic form of the data is modified most strongly. It is necessary that the experimenter understand in what ways the data are modified by the complete data system.

Present spacecraft systems are capable of collecting very large quantities of data. The experimenter must remember that his role is to gain a greater understanding of the physical universe, not merely to act as an efficient gatherer of data. He must require that his instruments operate as efficiently as possible to assist him in this role. This implies that he will employ automatic data processing techniques to the limit of the currently available technology, both in the spacecraft and on the earth for those processes which do not actually require his human judgment.

REFERENCES

1. Whitesitt, J. E., "Boolean Algebra and its Applications," Reading, Mass.: Addison-Wesley, 1961
2. Ludwig, G. H., "Cosmic-Ray Instrumentation in the First U. S. Earth Satellite," *Rev. Scient. Instr.* 30(4):223-229, April 1959
3. Suomi, V. E., "The Thermal Radiation Balance Experiment on Board Explorer VII," Juno II Summary Project Report, Marshall Space Flight Center Report MTP-M-RP-60-1, 1960, Ch. LL
4. Ludwig, G. H., "The Development of a Corpuscular Radiation Experiment for an Earth Satellite," State Univ. of Iowa Res. Rept. SUI-60-12, 1960
5. Ludwig, G. H., and W. A. Whelpley, "Corpuscular Radiation Experiment of Satellite 1959 Iota (Explorer VII)," *J. Geophys. Res.* 65(4):1119-1124, April 1960
6. Desai, U. D., Van Allen, R. L., and Porreca, G., "Eight-Level Pulse-Height Analyzer for Space Physics Applications," NASA Tech. Note D-666, January 1961
7. McIlwain, C. E., "Scintillation Counters in Rockets and Satellites," *IRE Trans. on Nuclear Sci.* NS-7(2-3):159-164, June-September 1961
8. Freeman, John W., "A Satellite Borne Cadmium Sulfide Total Corpuscular Energy Detector," State Univ. of Iowa Res. Rept. SUI-61-2, 1961
9. Richter, H. L., Jr., W. Pilkington, J. P. Eyraud, W. S. Shipley, and L. W. Randolph, "Instrumenting the Explorer I Satellite," *Electronics* 32(6):39-43, February 6, 1959
10. Ludwig, G. H., "The Instrumentation in Earth Satellite 1958 Gamma," IGY Satellite Rept. No. 13: 31-93, January 1961, U. S. National Academy of Sciences.
11. Mueller, G. E., "Telebit — An Integrated Space Navigation and Communication System," *Astronautics* 5(5):26-27, May 1960

12. International Telephone and Telegraph Corporation, eds., Reference Data for Radio Engineers, 4th ed., New York: American Book-Stratford Press, 1956
13. Rechtin, E., "Deep-Space Communications, Part I-Feasibility," *Astronautics* 6(4):37, April 1961
14. Mueller, G. E., "A Pragmatic Approach to Space Communication," *Proc. IRE* 48(4):557-566, April 1960
15. Smith, A. G., "Extraterrestrial Noise as a Factor in Space Communications," *Proc. IRE* 48(4):593-599, April 1960
16. Sanders, R. W., "Communication Efficiency Comparison of Several Communication Systems," *Proc. IRE* 48(4):575-588, April 1960
17. Viterbi, A. J., "On Coded Phase-Coherent Communications," *IRE Trans. on Space Electronics and Telemetry* SET-7(1):3-14, March 1961
18. Richter, H. L., Jr., "Microlock: A Minimum Weight Instrumentation System for a Satellite," Jet Propulsion Lab. External Publ. No. 376, April 15, 1957

